

Maladaptive positive feedback production of ChREBP β underlies glucotoxic β -cell failure

Received: 16 December 2021

Accepted: 18 July 2022

Published online: 30 July 2022

 Check for updates

Liora S. Katz¹, Gabriel Brill², Pili Zhang¹, Anil Kumar³, Sharon Baumel-Alterzon¹, Lee B. Honig¹, Nicolás Gómez-Banoy⁴, Esra Karakose¹, Marius Tanase¹, Ludivine Doridot⁵, Alexandra Alvarsson^{1,6}, Bennett Davenport⁷, Peng Wang¹, Luca Lambertini¹, Sarah A. Stanley¹, Dirk Homann¹, Andrew F. Stewart¹, James C. Lo⁴, Mark A. Herman^{8,9}, Adolfo Garcia-Ocaña¹ & Donald K. Scott¹ ✉

Preservation and expansion of β -cell mass is a therapeutic goal for diabetes. Here we show that the hyperactive isoform of carbohydrate response-element binding protein (ChREBP β) is a nuclear effector of hyperglycemic stress occurring in β -cells in response to prolonged glucose exposure, high-fat diet, and diabetes. We show that transient positive feedback induction of ChREBP β is necessary for adaptive β -cell expansion in response to metabolic challenges. Conversely, chronic excessive β -cell-specific overexpression of ChREBP β results in loss of β -cell identity, apoptosis, loss of β -cell mass, and diabetes. Furthermore, β -cell “glucolipotoxicity” can be prevented by deletion of ChREBP β . Moreover, ChREBP β -mediated cell death is mitigated by overexpression of the alternate CHREBP gene product, ChREBP α , or by activation of the antioxidant Nrf2 pathway in rodent and human β -cells. We conclude that ChREBP β , whether adaptive or maladaptive, is an important determinant of β -cell fate and a potential target for the preservation of β -cell mass in diabetes.

All major forms of diabetes arise from insufficient β -cell mass. Thus, extensive research efforts are underway to either preserve or expand functional β -cell mass^{1,2}. Under physiological conditions, increased blood glucose acts as a systemic adaptive β -cell mitogen, expanding functional β -cell mass through the proliferation of β -cells to meet demand for insulin³. However, prolonged hyperglycemia gives rise to glucose toxicity, which impairs insulin production and secretion, promoting a vicious cycle with ever-increasing glucose concentrations and ever-declining β -cell function, and eventually β -cell death⁴. Thus, depending on concentration and duration, increased blood glucose may drive either adaptation or diabetic pathogenesis.

Carbohydrate response-element binding protein (ChREBP, gene name *MLXIPL*) is a glucose-responsive transcription factor, originally cloned from liver, but also expressed at similar levels in pancreatic β -cells^{5,6}. A major target gene of ChREBP is thioredoxin interacting protein (Txnip), which binds to and inhibits the antioxidant enzyme, thioredoxin (Txn), thereby promoting oxidative damage in β -cells. Depletion of ChREBP prevents, and overexpression of Txnip promotes glucose toxicity and glucose-mediated β -cell death⁷. In contrast to these observations, our group found that ChREBP is necessary for glucose-stimulated β -cell proliferation, a critical process for adaptive expansion of β -cells. Furthermore, overexpression of the full-length

¹Diabetes, Obesity and Metabolism Institute, Icahn School of Medicine at Mount Sinai, One Gustave L. Levy Place, Box 1152 New York 10029, USA.

²Pharmacologic Sciences Department, Stony Brook University, Stony Brook, NY, USA. ³Metabolic Phenotyping Core, University of Utah, 15N 2030 E, 585, Radiobiology building, Room 151, Salt Lake City, UT 84112, USA. ⁴Weill Center for Metabolic Health and Division of Cardiology, Department of Medicine, Weill Cornell Medicine, New York, NY 10021, USA. ⁵Institut Cochin, Université de Paris, INSERM, CNRS, F-75014 Paris, France. ⁶Alpenglow Biosciences, Inc., 98103 Seattle, WA, USA. ⁷12800 East 19th Ave, Anschutz Medical Campus, Room P18-9403, University of Colorado, Aurora, CO 80045, USA. ⁸Division of Endocrinology and Metabolism and Duke Molecular Physiology Institute, Duke University Medical Center, Durham, NC, USA. ⁹Section of Diabetes, Endocrinology, and Metabolism, Baylor College of Medicine, One Baylor Plaza, MS: 185, R614, 77030 Houston, TX, USA. ✉e-mail: donald.scott@mssm.edu

form of ChREBP, now known as ChREBP α , does not cause β -cell death, but rather augments glucose-stimulated β -cell proliferation^{5,8}. These apparently disparate observations may be explained by expression and function of the different isoforms of ChREBP.

There are two major isoforms of ChREBP, ChREBP α and ChREBP β . Both are expressed in β -cells, as they are in adipocytes and hepatocytes^{9,10}. ChREBP β mRNA is transcribed from an alternative promoter located -17,000 bp upstream of the ChREBP α transcription start site and is alternatively spliced and translated so that ChREBP β lacks the low glucose inhibitory domain (LID) and nuclear export signal (NES) of the canonical full-length ChREBP α (Supplementary Fig. 1a). Thus, ChREBP β is constitutively active and nuclear, and orders of magnitude more transcriptionally potent than ChREBP α ¹¹. Importantly, ChREBP β expression is driven by powerful carbohydrate response elements (ChoREs) located near its own alternative transcription start site^{10–12}. Therefore, increased glucose metabolism activates ChREBP α and, if sustained, initiates a vigorous positive feedback loop, with the newly synthesized ChREBP β binding to its own ChoRE, producing more and more ChREBP β (Supplementary Fig. 1b). Gain- and loss-of-function experiments in vitro and ex vivo revealed that the induction of ChREBP β is the molecular engine that drives glucose-stimulated β -cell proliferation¹⁰. One goal of the present study was to test whether this process is necessary for the adaptive expansion of β -cells following a high-fat diet.

ChREBP β is expressed at high levels in diabetes, and overexpression of ChREBP β or a close homologue of ChREBP β that lacks the low glucose inhibitory domain and is thus constitutively active results in cell death of cultured β -cells^{10,13,14}. Thus, the molecular engine that drives glucose-stimulated β -cell transcription may also mediate cell death when levels of ChREBP β get too high. By contrast, overexpression of ChREBP α does not cause β -cell death because it stimulates the Nrf2 antioxidant pathway, delivering protection from oxidative damage^{8,15}. Despite these recent advances, key questions and controversies remain on the roles of the two ChREBP isoforms. For example, how is it that loss of ChREBP [presumably both isoforms¹⁶] and overexpression of ChREBP α ⁸ are both protective in settings of β -cell oxidative stress? Similarly, Shalev and colleagues found that acute overexpression of ChREBP β decreases ChREBP α expression, and hypothesized that ChREBP β is expressed at high levels in diabetes to block the presumed destructive effects of ChREBP α in diabetes¹³, a model clearly different from the one described above.

Here we clarify the roles of the ChREBP isoforms in β -cells using a variety of tools and in vitro and in vivo approaches that distinguish the two isoforms. We find that under conditions of high concentrations of glucose, high-fat diet, or diabetes, ChREBP β becomes the predominant isoform found in the nucleus of β -cells. Furthermore, we found that a modest, physiological induction of ChREBP β is necessary for adaptive proliferation and expansion of β -cells after a high-fat diet. However, robust β -cell-specific overexpression of ChREBP β mimics glucose toxicity in vivo, and results in frank diabetes. In addition, we find that deletion of ChREBP β prevents β -cell glucolipotoxicity. Finally, we present novel approaches to mitigate the effects of ChREBP β -mediated toxicity in rodent and human β -cells, providing insights for possible future therapies to preserve β -cell mass and combat type 2 diabetes. These observations place ChREBP isoforms at a nexus of control of the β -cell response to metabolic challenge and provide a revised understanding of glucolipotoxicity.

Results

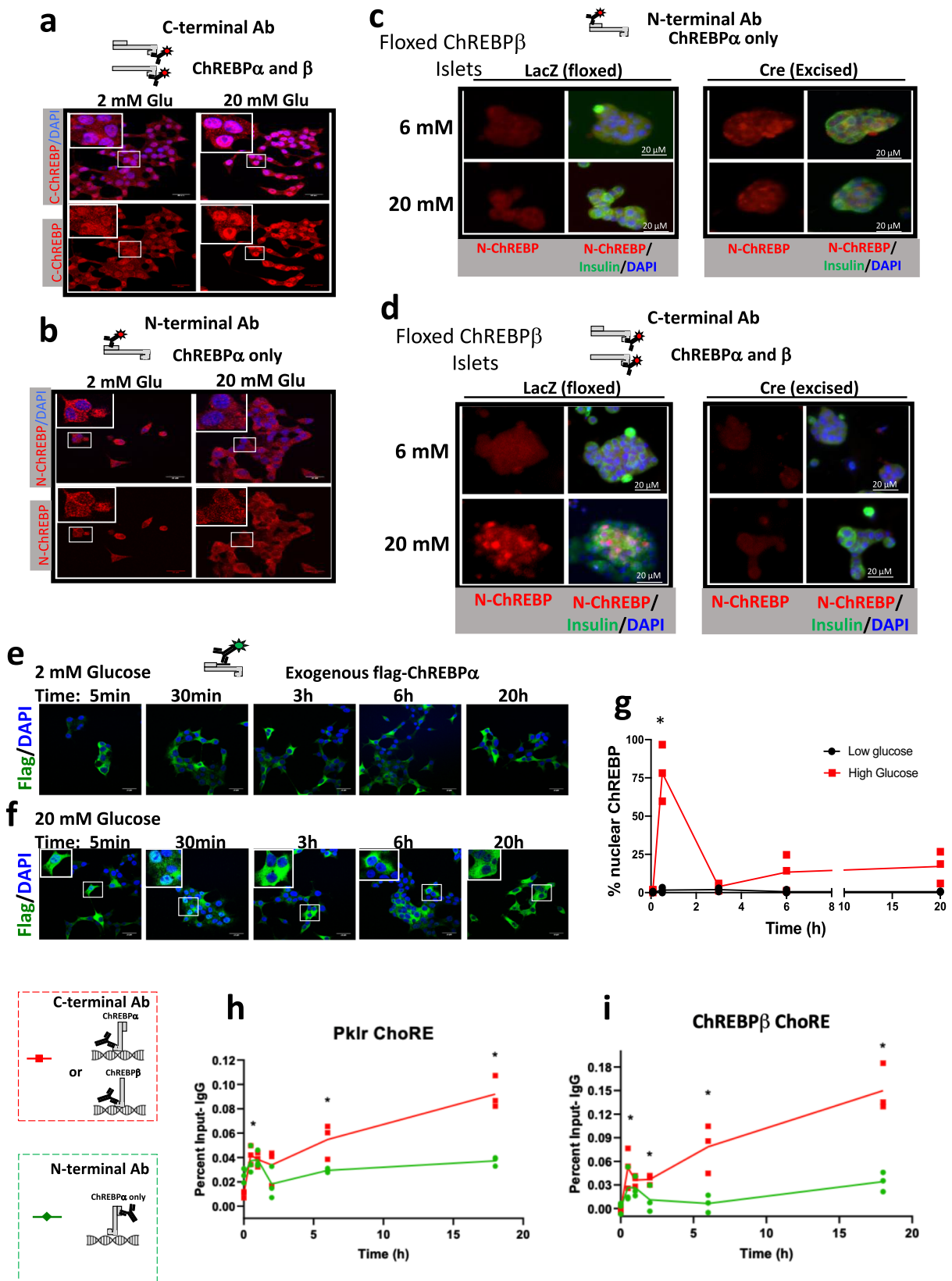
ChREBP β is the predominant nuclear isoform after prolonged exposure to high glucose

To understand the mechanisms and consequences of the dynamic relationship between activation of ChREBP α and the positive feedback induction of ChREBP β (Supplementary Fig. 1), it was critically important to devise and use tools that distinguish the two isoforms

(Supplementary Fig. 2). Since ChREBP β is a truncated version of ChREBP α , and lacks the N-terminal low glucose inhibitory (LID) domain¹¹, an antibody directed against an N-terminal epitope identifies only ChREBP α , and an antibody directed against the C-terminal region recognizes both ChREBP α and ChREBP β (Supplementary Figs. 1–3). We found ChREBP in the nucleus of INS-1-derived 832/13 cells (hereafter INS-1 cells), as expected, using an antibody recognizing the C-terminus and thus both isoforms after 24 h in 20 mM glucose (Fig. 1a), consistent with prior reports^{17,18}. Interestingly, when we used an N-terminal antibody, ChREBP α appeared mostly cytoplasmic, with no discernable difference between low and high glucose (Fig. 1b). Thus, the predominant nuclear ChREBP isoform was ChREBP β , which seemed at odds with the canonical view that ChREBP α translocates to the nucleus in response to increased glucose metabolism¹⁹. To confirm that ChREBP β was the nuclear isoform, we employed islets from floxed ChREBP β mice¹⁰. Dispersed islet cells transduced with either an adenovirus expressing LacZ, as a control, or Cre recombinase to remove ChREBP β , were incubated in 6 or 20 mM glucose for 48 h. As seen in Fig. 1c, d, the N-terminal antibody (ChREBP α) was mostly cytoplasmic, even in 20 mM glucose, while the C-terminal antibody showed bright nuclear staining after culture in 20 mM glucose, indicating the nuclear presence of ChREBP β . Importantly, after Cre-mediated deletion of ChREBP β , there was no nuclear ChREBP immunolabeling. To examine this further, we performed a time course experiment with adenovirally-expressed Flag-tagged ChREBP α , and an antibody against the Flag epitope in INS-1 cells after exposure to 2 or 20 mM glucose (Fig. 1e, f). Flag-tagged ChREBP α was mostly cytoplasmic when cultured in 2 mM glucose. After replacing the media with 20 mM glucose, Flag-tagged ChREBP α migrated rapidly into the nucleus within 5 min, in concert with previous observations^{17,18}. However, after 3 h in 20 mM glucose ChREBP α appeared cytoplasmic, and remained cytoplasmic at 6 and 24 h (Fig. 1f, g). These studies illustrate that ChREBP α moves transiently into the nucleus in response to glucose stimulation, but rapidly returns (minutes) to the cytoplasm. In contrast, ChREBP β , induced by high glucose via ChREBP α , becomes both elevated and nuclear.

To determine whether ChREBP β becomes the major isoform bound to DNA, we performed a time course chromatin immunoprecipitation (ChIP) experiment using antibodies directed against either the N-terminus (recognizing ChREBP α only) or the C-terminus (recognizing both isoforms; Supplementary Fig. 3). We selected the mouse *Pknox1* promoter as a target because it contains a well-studied ChoRE^{5,12,20,21}. The recruitment over time of ChREBP α to both the *Pknox1* ChoRE region and the ChREBP β (*Mlxip1*) ChoRE region increased for the first 30 min, and sharply decreased and plateaued for the remainder of the experiment (Fig. 1h, i). The recruitment of both isoforms, as determined by the C-terminal antibody, increased and decreased, similar to the signal from the N-terminal antibody, but then increased for the duration of the 18 h experiment. These observations strongly suggested that recruitment of ChREBP β continued throughout the time course of the experiment, whereas recruitment of the ChREBP α isoform increased only during the first 30 min of glucose treatment, broadly consistent with the experiments in Fig. 1a–f. These results are consistent with a model in which ChREBP β becomes the major nuclear ChREBP isoform bound to DNA after prolonged exposure to high concentrations of glucose. Together, these observations strongly suggest that ChREBP α is transiently nuclear, and that ChREBP β is the primary nuclear isoform after prolonged treatment with high concentrations of glucose.

An alternative explanation of the results in Fig. 1 could be that the epitope of the N-terminal antibody (recognizing only ChREBP α) becomes “masked” by the assembly of the transcriptional apparatus. In this scenario, the glucose-dependent recruitment of large co-activator protein complexes might sterically hinder the binding of antibodies, rendering ChREBP α “invisible”. To address this possibility, we used CRISPR/Cas9 editing to add fluorescent tags to the 5' and 3' ends of



full-length ChREBPα in INS-1 cells. mCherry was attached to the N-terminal LID domain, which identifies ChREBPα exclusively (Red cells, see schematic Fig. 2a). We also generated cells labeled with eGFP on the C-terminus (Green cells), representing both ChREBPα and ChREBPβ, and doubly labeled cells (Red/Green cells), in which ChREBPα appeared red/green, and ChREBPβ appeared green. The cells

were FACS sorted and validated via PCR, RT-PCR and Western blots (Supplementary Figs. 4–6). Red and Green cells were cultured in increasing concentrations of glucose (2–20 mM) for 72 h. Live-cell imaging demonstrated cytoplasmic localization for the ChREBPα regardless of glucose concentration, and nuclear localization for ChREBPβ at the highest concentration (Fig. 2b–d; Supplementary

Fig. 1 | ChREBP β is the main nuclear isoform after prolonged exposure to high concentrations of glucose. **a, b** Ins-1 cells were cultured in low (2 mM) or high (20 mM) glucose for 24 h. Cells were fixed and immunostained with the C-terminus antibody for ChREBP, which recognizes both ChREBP α and ChREBP β (**a**), or the N-terminus antibody for ChREBP, specific for ChREBP α (**b**). The results are representative of three independent experiments. **c, d** Islets from floxed ChREBP β mice were isolated and transduced with adenoviruses expressing LacZ as a control, or Cre recombinase to excise ChREBP β and cultured in 6 mM or 20 mM glucose. After 48 h, cells were fixed and immunostained with the N-terminal (**c**) or C-terminal (**d**) antibody; nuclei were stained with DAPI. Shown is a representative result of 3 independent experiments. **e, f** Ins-1 cells were transduced with an adenovirus

expressing flag-tagged ChREBP α and treated with 2 mM (**e**) or 20 mM glucose (**f**) for the indicated times. Cells were fixed and immunostained with an anti-Flag antibody and nuclei were stained with DAPI. The results from (**f**) were quantified in (**g**). The results are representative of three independent experiments, *, mean, $P < 0.05$. **h, i** Ins-1 cells were cultured overnight in 2 mM glucose and then glucose was added to a total of 20 mM for the indicated times; chromatin was isolated and processed for chromatin immunoprecipitation using antibodies recognizing the C-terminus, the N-terminus, or IgG. DNA was amplified by qPCR using primers specific for regions near the ChoREs on the *Pklr* (**h**), or *Mlxipl* (ChREBP β) (**i**) gene promoters. The data are the means \pm SEM of the percent input after subtraction of the IgG control. $n = 4$; * $p < 0.05$; *** $P < 0.0005$; **** $P < 0.0001$ using two-way ANOVA.

Fig. 7), independently confirming the results in the preceding paragraphs.

We next performed time-lapse confocal microscopy in INS-1 cells bearing fluorescent tags on both ends of ChREBP (Red/Green cells), while culturing the cells in 2 mM or 20 mM glucose, or after transitioning the cells from low to high glucose. We quantified the nuclear localization of red fluorescence (representing ChREBP α) and exclusively green fluorescence (representing ChREBP β). After culture for 24 h in 2 mM glucose, nearly all of the fluorescence was cytoplasmic (Fig. 2e, f, left panels). Culture in 20 mM glucose for 24 h resulted in predominantly green nuclear fluorescence, indicating ChREBP β as the principal nuclear form (Fig. 2e, f right panels). The green signal (ChREBP β) was mostly nuclear throughout the time of acquisition. In contrast, the red signal (ChREBP α) was present in approximately 50% of the nuclei with a more random distribution, illustrating that ChREBP shuttles between the nucleus and the cytoplasm, and that increased glucose accelerates the rate of nuclear entry¹⁷. When the glucose in the medium was changed from 2 mM to 20 mM (Fig. 2e, f, middle panels), there was a rapid nuclear localization of ChREBP α (red and green fluorescence) followed by a separation of fluorescent signals after approximately 30 min, agreeing with our observations in Fig. 1 (and see Supplementary Fig. 8a and Supplementary Movie 1). Interestingly, we found that nuclear localization of either isoform required ongoing protein translation as it was inhibited by cycloheximide (Supplementary Fig. 8b). Together, these results suggested a model wherein ChREBP α is mostly cytoplasmic at low glucose, but with increased glucose metabolism, ChREBP α transiently becomes more nuclear to induce the production of ChREBP β . ChREBP β remains predominantly nuclear due to the absence of the LID domain (including the NES) and is more potently and constitutively active when compared to ChREBP α ¹¹. With sustained high levels of glucose, this positive feedback mechanism continues to produce more ChREBP β , ensuring that ChREBP β becomes the major isoform recruited to ChoREs (Supplementary Fig. 1b).

ChREBP β expression and nuclear localization correlate with hyperglycemia and diabetes

ChREBP β was visualized in the nucleus of mouse β -cells in vivo, using our validated C-terminal antibody approach under quiescent, metabolically stressful, and diabetic conditions (Fig. 3a). The N-terminal antibody, representing ChREBP α only, was mostly cytoplasmic in all the conditions tested (Fig. 3a). In C57BL/6 mice, we observed a gradation of ChREBP β expression: no detectable expression on a standard chow diet; modest abundance after one week on a high-fat diet, representing a normal physiological adaptive response¹⁰, and very high expression levels in diabetic *db/db* mice (Fig. 3a). In addition, human islets labeled with a RIP-ZsGreen-expressing adenovirus were sorted to obtain pure β -cells²². The ratio of ChREBP β to ChREBP α mRNA expression was significantly higher in subjects with T2D compared to non-diabetic control donors (Fig. 3b). Furthermore, we found that treatment of *db/db* mice with adipisin, which preserves β -cell mass in diabetic *db/db* mice²³, decreased ChREBP β abundance in a manner

proportionate to the improved glycemia and plasma insulin levels, concordant with the idea that ChREBP β expression contributes to the glucose toxicity seen in the *db/db* mouse model of T2D (Fig. 3c–f).

We next explored nuclear localization of ChREBP β in human β -cells in vivo using a minimal human islet transplant model in immunosuppressed mice²⁴. In this experiment, human islets were transduced with adenoviruses and then transplanted under the kidney capsules of streptozotocin-induced diabetic immunocompromised mice (Fig. 4a). 1500 islet equivalents (IEQs) were sufficient to normalize glucose levels (Fig. 4b). 500 IEQs transduced with a control Cre-expressing adenovirus was a minimal mass of β -cells sufficient to keep the animals alive, but hyperglycemic (around 400 mg/dL). When 500 IEQs were transduced with an adenovirus expressing ChREBP α , which activates the Nrf2 antioxidant pathway⁸, blood glucose, plasma insulin, and glucose tolerance all approached normal levels (Fig. 4b–e). At the end of the experiment, a uninephrectomy was performed and glucose levels rose to diabetic levels, confirming that the transplanted human β -cells provided the only insulin in the recipient mice (Fig. 4b). Kidneys containing islet grafts were fixed and immunolabeled for insulin and ChREBP using the C-terminal antibody (Fig. 4f). This revealed abundant nuclear ChREBP β in β -cells transduced with control, Cre-expressing adenovirus, but nuclear labeling was nearly absent in the ChREBP α -treated β -cells. In addition, there was a strong correlation between glucose levels prior to the harvesting of the graft and nuclear ChREBP β abundance (Fig. 4g). Thus, nuclear ChREBP β expression is proportionate to glucose levels in human β -cells in vivo.

Whereas ChREBP β is required for adaptive β -cell proliferation and expansion of β -cell mass, depletion of ChREBP β protects from glucolipotoxicity

To more deeply explore the physiological role of ChREBP β in adult pancreatic β -cells, floxed ChREBP β ^{lox/lox} mice were crossed with MIP-Cre-ERT mice to generate a β -cell-specific tamoxifen-inducible knock out of ChREBP β (*i* β KO β)^{10,25} (Fig. 5a and Supplementary Fig. 9, 10). *i* β KO β mice were injected with tamoxifen or oil for 5 consecutive days (75 μ g/g body weight). Two days later, they were placed on either a control chow diet or a high-fat diet (HFD) for either one or four weeks. As expected, the oil-injected mice showed nuclear ChREBP labeling with the C-terminal antibody after a high-fat diet, whereas this labeling was not observed in the tamoxifen-injected mice, confirming the high knock-out efficiency in *i* β KO β mice, and supporting the notion that ChREBP β becomes nuclear in vivo in response to high-fat feeding (Supplementary Fig. 9a). Three weeks after the first tamoxifen injection, mice on a HFD displayed a significant increase in non-fasting blood glucose levels compared to vehicle-treated littermate controls at 3 weeks (Fig. 5b). After one week, glucose tolerance was impaired on a HFD, but there was no significant difference between the oil and tamoxifen-injected groups (Fig. 5c, d). However, Ki67 immunolabeling in β -cells after one week on a HFD was significantly lower in tamoxifen-injected *i* β KO β mice compared to littermate controls, demonstrating the necessity for ChREBP β for adaptive β -cell proliferation (Fig. 5e, f). After 1 month on a HFD, the tamoxifen-injected mice became more

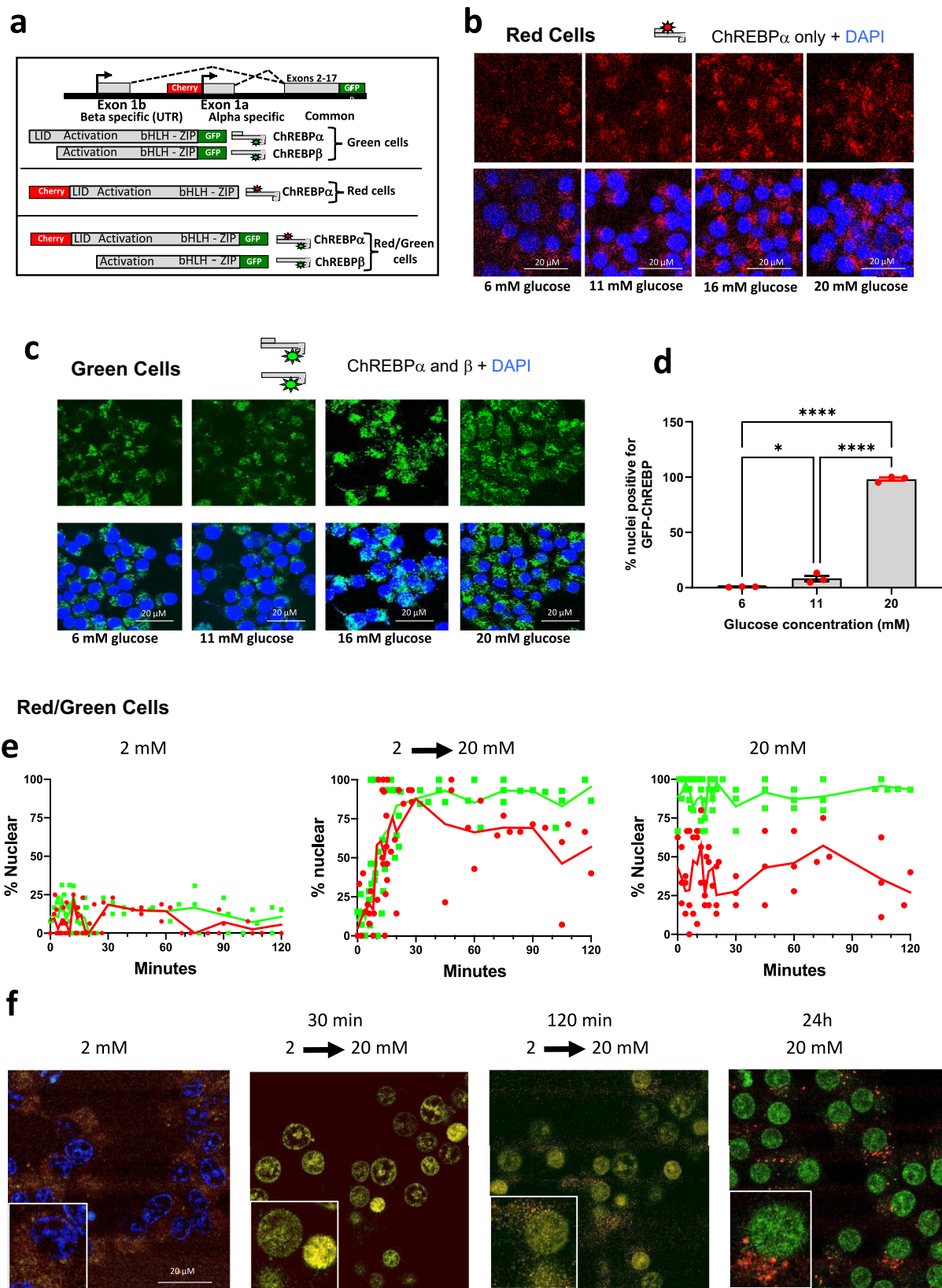


Fig. 2 | Cellular localization of genetically edited and tagged ChREBP isoforms in response to glucose. **a** Design of labeled ChREBP isoforms. mCherry and eGFP were integrated into the genome using the CRISPR/Cas9 method for gene editing in frame with exon 1a and exon 17. **b**, **c** Confocal live imaging was performed on Red or Green INS-1 cells after incubation with the indicated concentrations of glucose for 72 h. **d** The percent nuclear green fluorescence from **c** was determined. Data are the means \pm SEM, $n = 3$, $*P < 0.05$; $****p < 0.0001$ using one-way ANOVA. **e**, **f** Red/

Green INS-1 cells were incubated in 2 or 20 mM glucose or the media was changed from 2 to 20 mM glucose as indicated. Confocal live-image microscopy was performed and the percent nuclear green or red fluorescence was determined. The data presented in **(e)** represent the aggregate of 3 independent experiments. **f** Representative images from the indicated times and treatments. DAPI nuclear staining is included in the 2 mM image and excluded in the others for clarity. See also related Supplementary Figs. 4–8 and Supplementary Movie 1.

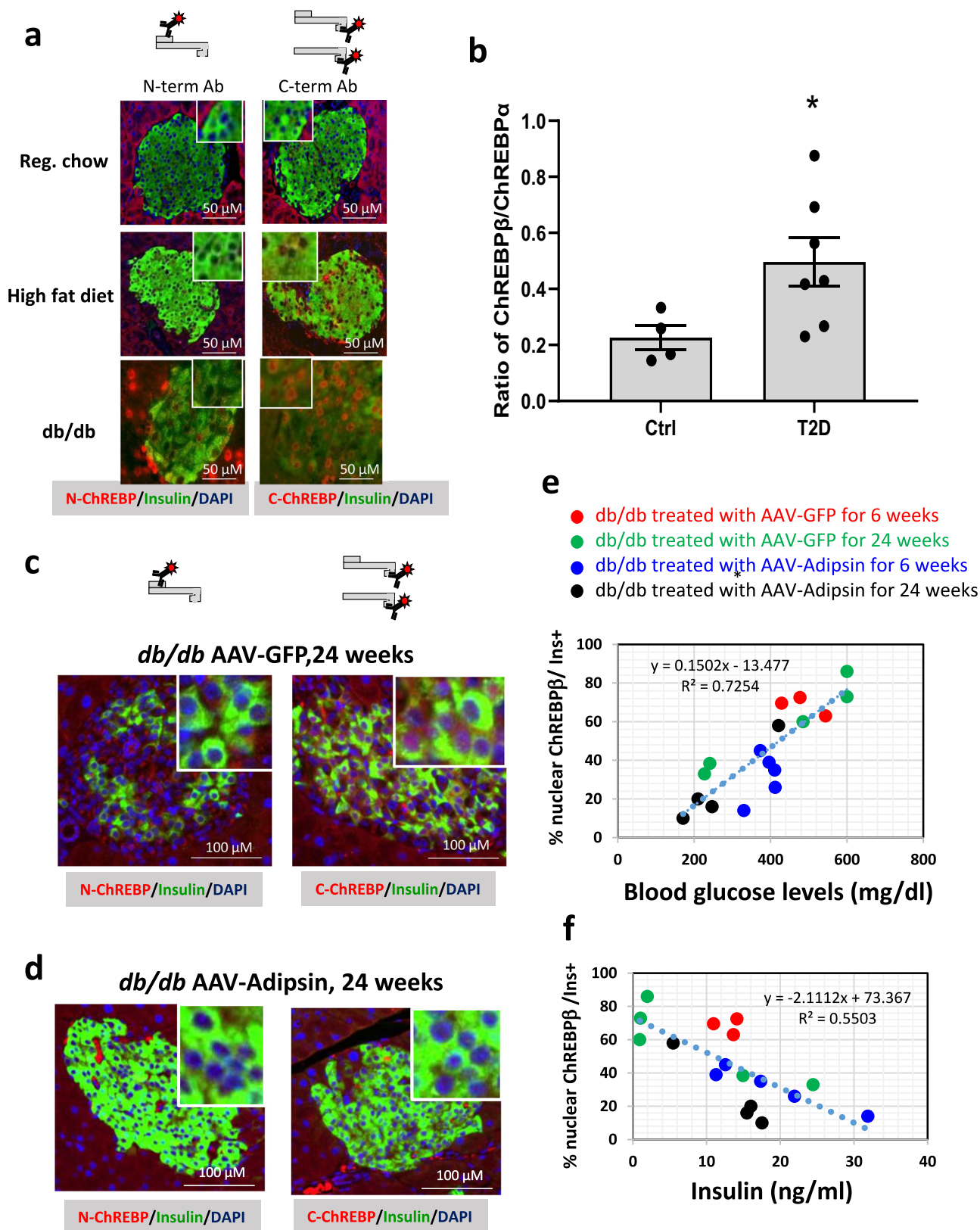
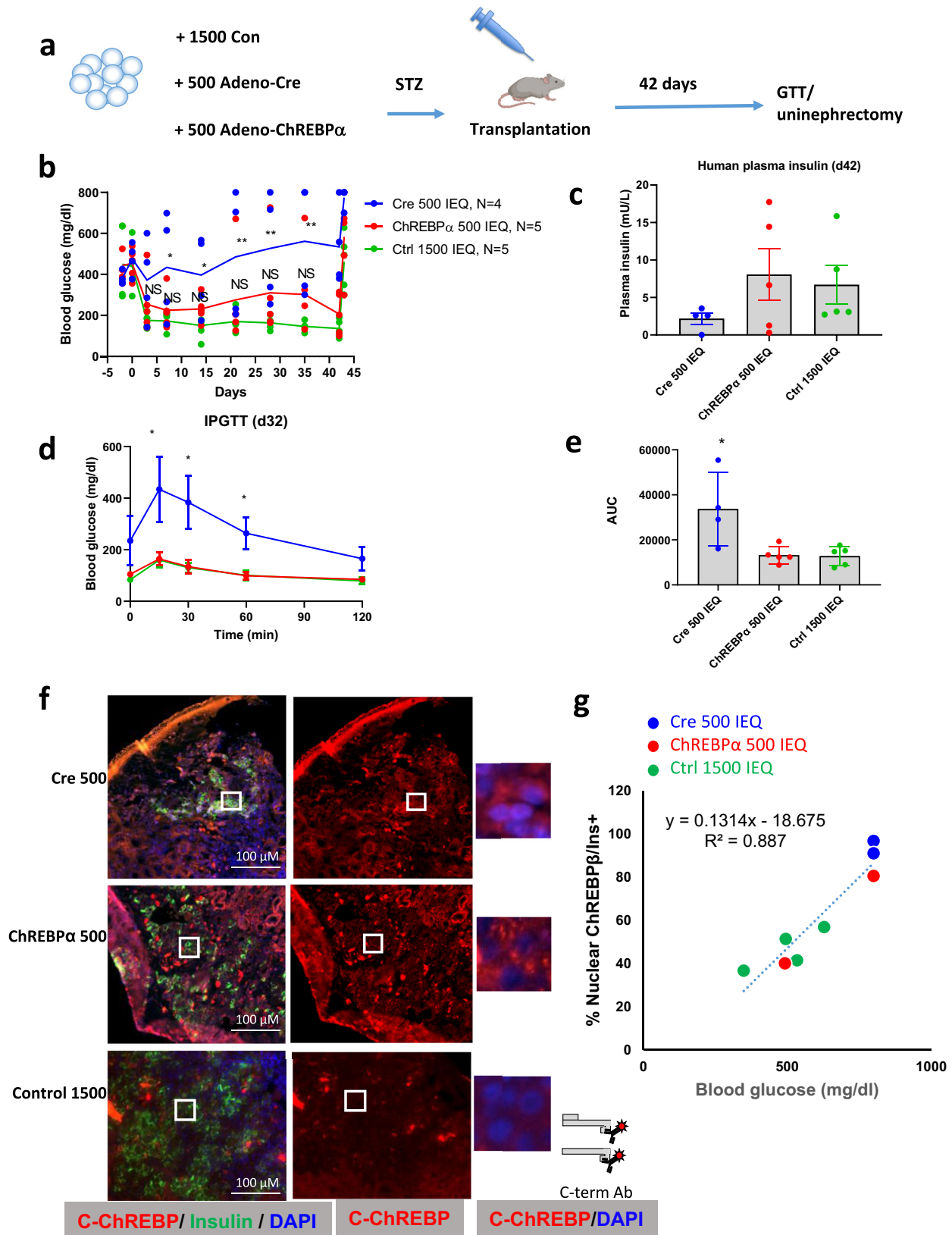


Fig. 3 | ChREBP β expression and nuclear localization correlates with adaptive expansion of β -cells and with glucose toxicity in diabetes. **a The N-terminal or the C-terminal antibodies recognizing ChREBP were used to immunolabel pancreatic tissue slices from C57Bl/6 mice fed on a standard chow diet, or fed a high-fat diet for 1 week, or from *db/db* diabetic mice. All micrographs represent at least 3 independent experiments. **b** Ratio of expression of ChREBP β to ChREBP α FPKM from RNAseq performed from FACS-sorted human β -cells isolated from non-diabetic ($n = 4$) and Type 2 diabetic subjects ($n = 7$). Each data point represents a different**

donor. Data are means \pm SEM; * $p < 0.05$ using one-way ANOVA. **c, d** The N-terminal or C-terminal antibody recognizing ChREBP were used to immunolabel pancreatic tissue slices from diabetic *db/db* mice treated with control AAV (GFP) or with AAV expressing adipsin for 24 weeks. Correlation between percentages of nuclear ChREBP β in insulin-positive β -cells and blood glucose levels (**e**) or blood insulin levels (**f**), where each data point represents an individual mouse. All micrographs represent at least 3 independent experiments.



glucose intolerant compared with littermate oil-injected mice (Fig. 5g, h). Concordantly, β -cell mass was significantly lower in tamoxifen-injected $i\beta$ KO β mice fed a HFD for a month compared to $i\beta$ KO β mice injected with oil and fed a HFD, but was not different from β -cell mass in chow-fed control mice (Fig. 5i). Plasma insulin levels remained the same in mice on a HFD diet despite the increased glucose levels

(Fig. 5j). Female mice were largely protected from the effects of ChREBP β depletion (Supplementary Fig. 10c–g). Together, these findings illustrate that ChREBP β is necessary for adaptive β -cell mass expansion.

We repeated these experiments, crossing ChREBP $\beta^{lox/lox}$ mice with INS-1-Cre^{Herr} mice²⁶, which express Cre under control of the insulin

Fig. 4 | ChREBP β nuclear localization correlates with blood glucose levels in β -cells from transplanted human islets. **a** Schematic of experimental design using the STZ-diabetic immunocompromised marginal islet mass model (Created with BioRender.com). Three groups of mice each received human islets from the same four to five human islet donors: Cre-transduced 500 IEQs ($n = 4$), ChREBP α -transduced 500 IEQs ($n = 5$), or 1500 untreated control IEQs ($n = 5$). The 500 IEQ groups were treated with an adenovirus expressing either Cre as a negative control or ChREBP α 24 h prior to transplantation. Glucose tolerance test was performed at day 42, a unilateral nephrectomy was performed at day 43. **b** Glucose levels were

measured. **c** Circulating insulin measured using a human insulin-specific assay. **d** Intraperitoneal glucose tolerance test. **e** Area under the curve (AUC) for the three groups in **(d)**. Values are means \pm SEM. * $p < 0.05$; ** $p < 0.01$ compared to 1500 IEQ using two-way ANOVA. **f** Representative images of insulin and C-terminal ChREBP immunohistochemistry from islet grafts of at least 3 different mice. **g** Correlation between percentages of nuclear ChREBP β from at least 1000 insulin-positive β -cells from the grafted human islets and blood glucose levels, where each data point represents an individual transplanted mouse.

promoter at or near embryonic day 8.5, to generate an embryonic β -cell-specific knock out of ChREBP β (e β KO β), and performed the same set of experiments on two-month-old mice (Supplementary Figs. 11–13). These experiments recapitulated the results in i β KO β mice, showing that ChREBP β was necessary for β -cell expansion after a HFD in male (but not female) mice. Thus, ChREBP β is dispensable for normal β -cell development under non-metabolically-stressed conditions, but is required for adaptive proliferation and expansion of β -cell mass in response to a HFD in adult male mice.

To explore underlying mechanisms, mRNA was isolated from islets of male e β KO β mice fed one week on a chow or HFD (Supplementary Fig. 12e–g). Whereas the knockdown efficiency of ChREBP β in the Cre-positive mice both on chow or HFD is evident and significant, ChREBP α remained unchanged between Cre-negative and Cre-positive groups, as did β -cell markers, consistent with the idea that ChREBP β is not necessary for β -cell differentiation or maintenance of β -cell phenotype. Myc, a cell cycle regulator required for adaptive expansion of β -cell mass, and an essential factor for ChREBP activity^{21,27,28}, was downregulated in both chow and HFD after depletion of ChREBP β (Supplementary Fig. 12g). This suggests that the lack of proliferation seen in Cre-positive i β KO β and e β KO β β -cells may be caused by a failure to induce Myc in response to the HFD. Altogether, the data from the i β KO β and e β KO β mice demonstrate that ChREBP β plays a key role in adaptive β -cell proliferation but is unlikely to play a role in normal pre- and postnatal β -cell expansion during development.

Depletion of ChREBP β protects against glucolipotoxicity

To further explore whether ChREBP β might play a role in glucolipotoxicity, we cultured dispersed islet cells from ChREBP $\beta^{\text{lox/lox}}$ mice after transduction with adenoviruses expressing either control GFP or Cre recombinase in low glucose or high glucose plus palmitate (Fig. 5k, l). Culturing islet cells in glucolipotoxic conditions led to marked increases in β -cell death as assessed using TUNEL assay (average ~50%). Strikingly, deletion of ChREBP β completely prevented cell death. Thus, although transient increases in ChREBP β are necessary for adaptive β -cell expansion, sustained increases in ChREBP β are a key driver of glucolipotoxic β -cell death.

ChREBP β overexpression in vivo results in β -cell death and diabetes

To test if overexpressing ChREBP β in β -cells caused β -cell death in vivo, MIP-Cre-ERT mice were crossed to mice containing a Lox-Stop-Lox Flag-tagged ChREBP β cassette residing in the *Rosa26* locus, termed i β OE β mice (Fig. 6a, Supplementary Fig. 14). Cre-mediated recombination resulted in the expression of flag-tagged ChREBP β , confirmed by immunoblots and RT-PCR. Tamoxifen-mediated recombination was restricted to β -cells (Supplementary Fig. 14b–d). Furthermore, immunostaining of pancreata displayed a marked induction of Cre in insulin-positive β -cells from the i β OE β mice after tamoxifen treatment (Supplementary Fig. 14e).

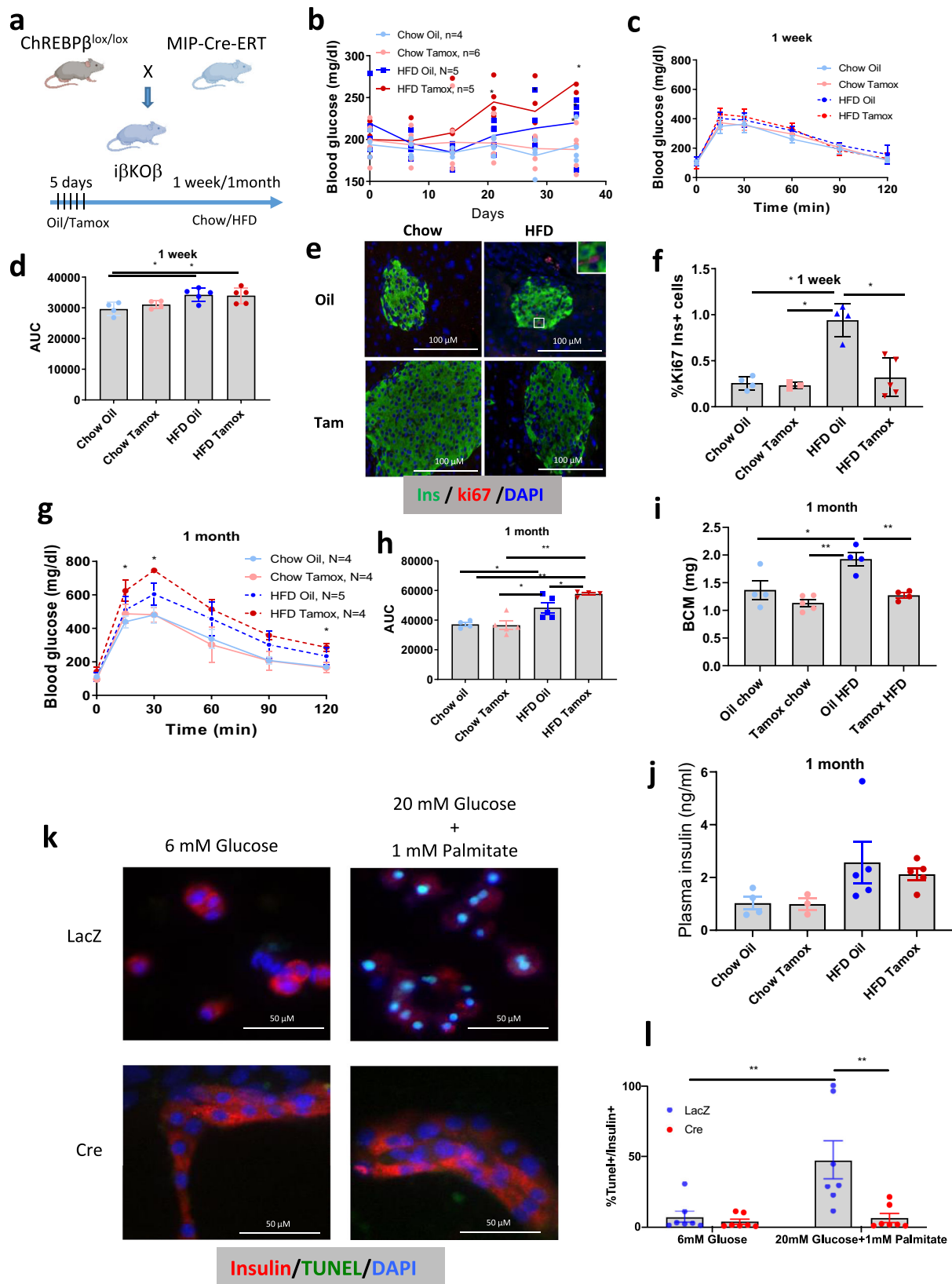
Seven days after tamoxifen-injection, i β OE β male mice displayed no significant change in glucose tolerance, body weight, plasma insulin or non-fasting glucose (Fig. 6b–f). However, heterozygotes and homozygotes displayed significant decreases in β -cell mass after one

week (Fig. 6g). Strikingly, within 30 days after the last injection of tamoxifen, male i β OE β mice became diabetic, evidenced by increased non-fasting blood glucose levels, impaired glucose tolerance and a marked decrease in β -cell mass, all in a gene-dose-dependent manner (Fig. 6f, h–j). Induction of ChREBP β was associated with a significant increase in Ki67 staining, and a concomitant increase in TUNEL staining, perhaps reflecting simultaneous attempts at β -cell proliferation and cell death, or DNA damage repair activity (Fig. 6k–n). By contrast, females were partially protected, with only homozygous mice displaying significant glucose intolerance one month after tamoxifen treatment, (Supplementary Fig. 15). Thus, inducible overexpression of ChREBP β in mice mimics glucose toxicity with β -cell destruction resulting in diabetes.

To determine whether ChREBP β impacts β -cell function if overexpressed early in development, Lox-Stop-Lox Flag-tagged ChREBP β mice were crossed with INS-1-Cre^{Herr} mice²⁶, to generate embryonically expressed β -cell-specific knock-in flag-tagged ChREBP β mice, termed e β OE β mice (Supplementary Figs. 16a–c). At 3 weeks of age, body weight was not significantly different between the Cre-negative and Cre-positive littermates, and only homozygous e β OE β mice showed a significant increase in non-fasting or fasting blood glucose levels (Supplementary Fig. 16d, e). By 8 weeks both heterozygous and homozygous e β OE β Cre-positive mice displayed increased non-fasting glucose levels (Supplementary Figs. 16e). At 8 weeks of age, the male mice overexpressing either one or two copies of ChREBP β had severely impaired glucose tolerance, increased fasting and non-fasting glucose levels, and homozygous animals had severe diabetes and weight loss (Supplementary Fig. 16d–h). Concordantly, insulin levels were significantly decreased in homozygous mice, and β -cell mass was nearly absent for both heterozygous and homozygous mice (Supplementary Fig. 16i, j). Furthermore, the islet architectures of the Cre-positive mice are clearly disturbed with necrotic centers evident within islets (Supplementary Fig. 17a), with no obvious difference in somatostatin or glucagon immunolabeling, and normal alpha cell mass (Supplementary Fig. 17b). The overall graded response between heterozygotes and homozygotes demonstrated a gene dosage effect. Insulin tolerance was very similar between the Cre-negative and Cre-positive groups, indicating that the diabetic phenotype was due to catastrophic loss of β -cell mass rather than insulin intolerance in peripheral tissues (Supplementary Fig. 17c–g; see also Supplementary Movies 2 and 3). Results in female e β OE β mice were similar to those in male mice (Supplementary Fig. 18). Thus prolonged and very high overexpression of ChREBP β leads to β -cell death, mimicking glucotoxicity.

Overexpression of ChREBP β promotes a signature of increased proliferation, apoptosis, and dedifferentiation

To more deeply explore the relationship between ChREBP β overexpression and β -cell proliferation versus death, we performed RNA-seq using INS-1 cells transduced with a control adenovirus (GFP) or an adenovirus overexpressing ChREBP β and cultured for 48 h in 2 mM or 11 mM glucose (Fig. 7). Six differential gene expression (DGE) analyses were conducted to unbiasedly compare all possible combinations between the 4 groups. Gene Ontology (GO) terms enriched by differentially expressed genes (Supplementary Table 4) from each DGE were



processed using the ViSEAGO R package that helps capture the biological background from the complexity of the experimental design with multiple comparisons²⁹. ViSEAGO computed the semantic similarity between 471 enriched GO terms, and identified 45 clusters, and 5 superclusters of GO terms (Fig. 7a). Supercluster (1) includes clusters populated by apoptosis, cell death and proliferation clusters. Other

superclusters include transmembrane transport (2) regulation of metabolic processes (3 and 4) and cell differentiation (5). Figure 7b depicts a volcano plot comparing GFP and ChREBP β -treated INS-1 cells cultured in 11 mM glucose. GO pathway analysis revealed that the top two pathways associated with ChREBP β overexpression in 11 mM glucose were proliferation and apoptosis (Fig. 7c). Nearly every apoptosis

Fig. 5 | ChREBP β is required for adaptive β -cell proliferation and expansion of β -cell mass, and loss of ChREBP β prevents glucolipotoxicity. **a** Schematic showing generation of β -cell specific, inducible ChREBP β knockout mice (i β KO β , created with BioRender.com). **b** Blood glucose levels after the indicated treatments and times. **c, d** Glucose tolerance test and area under the curve measurements after 1 week on a chow or high-fat diet (HFD). **e, f** Percent Ki67-positive/insulin-positive cells in pancreata from i β KO β mice after 1 week of HFD. **g, h** Glucose tolerance test and area under the curve measurements after 1 month on a chow or high-fat diet

(HFD). **i, j** β -cell mass and Plasma insulin were measured after 1 month on a chow or high-fat diet (HFD). Data are means \pm SEM; $N = 4$ or 5 as indicated; * $p < 0.05$; ** $p < 0.01$ using two-way ANOVA. **k** Islets were isolated from floxed ChREBP β mice, dispersed and transduced with adenoviruses expressing either GFP or Cre recombinase. Cells were cultured as indicated and subjected to a TUNEL assay after 48 h and immunostained for insulin and DAPI. **l** Percentage of insulin-positive/TUNEL-positive cells. Data are means \pm SEM; $N = 7$; * $p < 0.05$; ** $p < 0.01$ using two-way ANOVA.

marker was upregulated by ChREBP β , both in 2 mM and 11 mM glucose (Fig. 7d). In addition, *Txnip*, which drives β -cell glucose toxicity and is a major target gene of ChREBP β ³⁰, was highly upregulated by ChREBP β in both 2 mM and 11 mM glucose (Fig. 7e). Key cell cycle regulator genes were generally induced by increased glucose, and overexpression of ChREBP β led to an even greater increase in their expression (Fig. 7f). By contrast, β -cell identity markers were markedly decreased by ChREBP β overexpression (Fig. 7g). Thus, overexpression of ChREBP β behaves much like overexpression of *Myc*, with a signature supporting both proliferation and apoptosis in β -cells, and with a general effect of decreasing β -cell identity while increasing the transcription of most of the genes examined^{31,32}.

Rescue from ChREBP β -mediated β -cell death by ChREBP α and Nrf2

Since overexpression of ChREBP α does not result in β -cell death, but rather augments glucose-stimulated β -cell proliferation via activation of the antioxidant Nrf2 pathway^{5,8}, we queried whether co-expression of ChREBP α with ChREBP β could rescue β -cells from ChREBP β -mediated cell death. We first tested the hypothesis that the ratio of ChREBP α :ChREBP β is an important determinant of β -cell apoptosis. INS-1 cells were transduced with a constant MOI (150) of adenoviruses expressing either ChREBP α or ChREBP β . Increasing MOIs of each virus were compared, using LacZ-expressing adenovirus to maintain a constant viral load (Fig. 8a). Cell death, as measured by Annexin V staining and flow cytometry, was evident when the ratio of ChREBP β to ChREBP α was greater than one. In addition, titration of ChREBP α into ChREBP β -expressing cells reduced β -cell death. We next isolated islets from *Lox-stop-Lox* ChREBP β mice, and induced ChREBP β using a Cre adenovirus in the absence or presence of an adenovirus expressing ChREBP α , and then measured β -cell death after 48 h by counting TUNEL- and insulin-positive cells. There was almost universal apoptosis in cells overexpressing ChREBP β , but co-expression of ChREBP α with ChREBP β rescued β -cell death (Fig. 8b, c). Overexpression of ChREBP α activates the antioxidant Nrf2 pathway⁵. Thus, we explored whether CDDO-Me, an Nrf2 activator, might also rescue β -cells from isolated ChREBP β -mediated cell death using islets from *Lox-stop-Lox* ChREBP β mice. This proved to be true (Fig. 8b, c). Thus, overexpression of ChREBP α or activation of Nrf2 rescues murine β -cells from the cytotoxicity of ChREBP β overexpression.

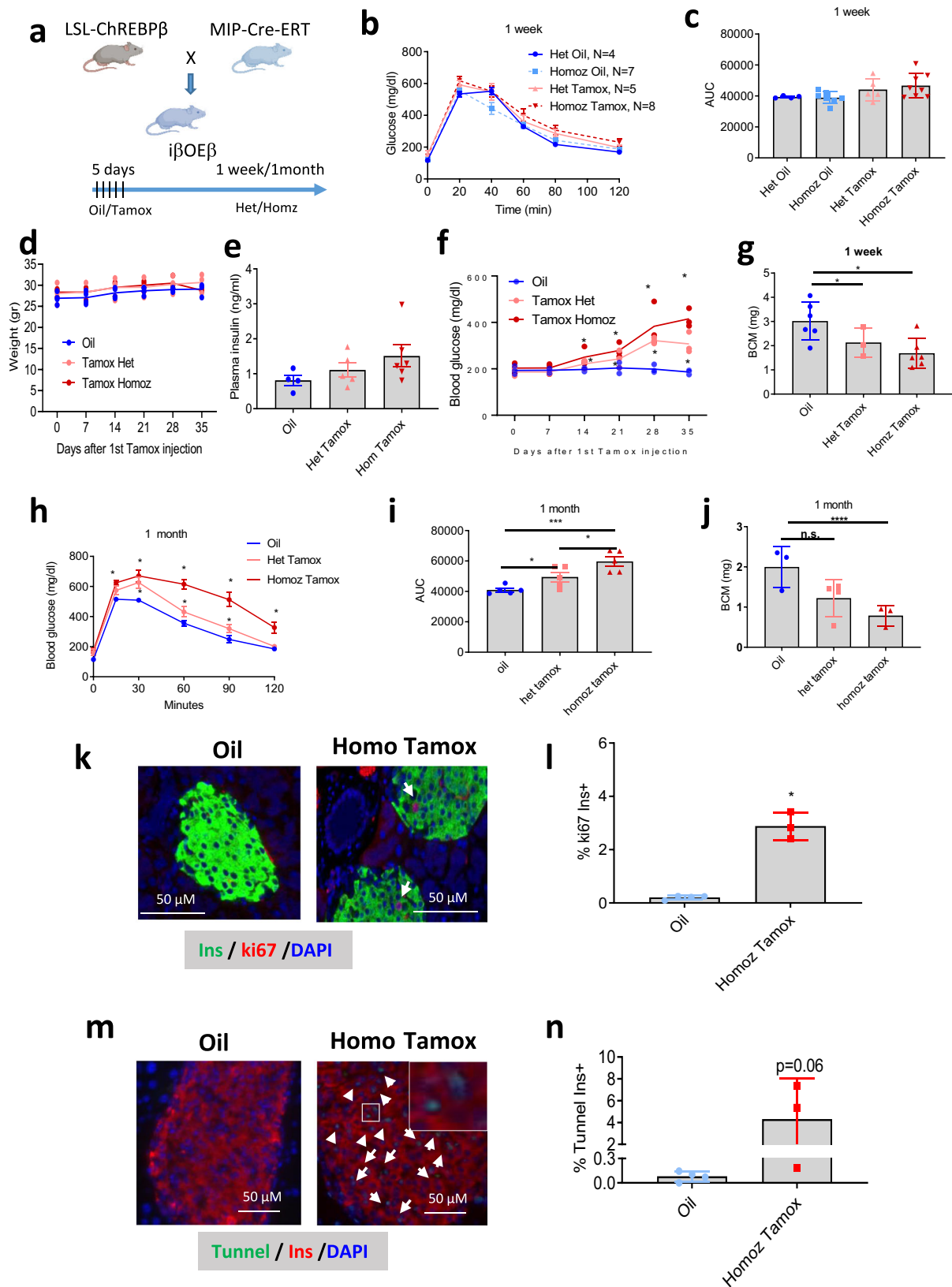
We asked if ChREBP α could rescue ChREBP β -mediated β -cell death in human β -cells. ChREBP β was overexpressed using an adenovirus in dispersed human islets. Overexpression of ChREBP β resulted in pronounced β -cell apoptosis, as assessed by insulin immunolabeling and TUNEL assay (Fig. 8d, e). We also immunolabeled the same cells for Ki67 and observed a marked Ki67 labeling in β -cells, likely reflecting DNA damage in dying β -cells [Fig. 8f; refs. 2,33]. Overexpression of ChREBP α had no effect on either proliferation or cell death. However, co-expression of ChREBP β and ChREBP α resulted in a complete absence of cell death, but retention of robust β -cell proliferation. In separate experiments, ChREBP β -transduced human islet cells were treated with CDDO-Me, an Nrf2 activator (Fig. 8e, f). CDDO-Me reduced ChREBP β -mediated TUNEL staining and induced or permitted robust Ki67 immunolabeling, strongly suggesting that the rescue effect of ChREBP α was at least in part due to activation of the Nrf2 antioxidant pathway.

Discussion

β -cells have the remarkable ability to adapt and compensate for increased demand for insulin by expanding β -cell mass, as happens in response to a hypercaloric Western diet in rodents or pregnancy in rodents and humans^{2,34}. Diabetes results from an inability of β -cells to compensate for increased demand for insulin, or from decompensation resulting from a glucotoxic environment from prolonged hyperglycemia^{135,36}. Here we find that ChREBP β is a key modulator of both compensation and decompensation of β -cells (Fig. 9). Major findings include: (1) in response to increased glucose, ChREBP α rapidly and transiently migrates to the nucleus, and through the resulting positive feedback induction, ChREBP β becomes the major nuclear form of ChREBP. The nuclear abundance of ChREBP β correlates with the degree of hyperglycemia in rodent and human β -cells. Thus, nuclear ChREBP β is a biomarker for the β -cell response to hyperglycemia. (2) The induction of ChREBP β is required for the normal early physiological adaptive expansion of β -cells in response to a high-fat diet. (3) Chronic ChREBP β overexpression results in β -cell death and diabetes. (4) Deletion of ChREBP- β prevents glucolipotoxicity in cultured mouse β -cells. (5) ChREBP- β -mediated glucose toxicity can be mitigated by exogenous expression of ChREBP α , or with activation of the Nrf2 antioxidant pathway.

The canonical view of ChREBP translocation posits that ChREBP remains in the cytoplasm under low glucose conditions, and then rapidly translocates to the nucleus in response to the metabolism of glucose¹⁹. Most assays that characterize ChREBP translocation have been performed either with antibodies that do not distinguish between ChREBP α and ChREBP β , or by ectopic expression of epitope-tagged ChREBP α ^{17,18,37}. Here we used tools designed to distinguish the two major endogenous isoforms and found that ChREBP α only transiently migrates to the nucleus in response to glucose and then induces the production of ChREBP β . Importantly, ChREBP β is generated from a powerful positive feedback loop driven by ChoREs near an alternative transcription start site. Alternative splicing replaces exon 1a with exon 1b, leading to a mRNA encoding ChREBP β that lacks the LID domain and an NES, and so is more transcriptionally potent and more likely to be nuclear than ChREBP α ¹¹. Thus, with sustained, prolonged glucose metabolism, ChREBP β becomes the predominant ChREBP isoform bound to DNA. The functional interaction between the two isoforms of ChREBP provides the molecular machinery for acute glucose regulation by ChREBP α , and the regulation of adaptive responses for longer exposure to glucose by ChREBP β , and the potential for pathological consequences after chronic and unrestrained positive feedback expression of ChREBP β .

While transcriptional regulation and localization of the two splice isoforms, as demonstrated in this study seem to be of high importance for the regulation of ChREBP and activity, there are additional mechanisms that have been previously shown to tightly regulate ChREBP location and activity. ChREBP is regulated by carbohydrate metabolites and other metabolic signals^{19,38}, including Ca^{2+} flux, which dissociates its binding to sorcin allowing nuclear translocation in beta cells¹⁸, and several posttranslational modifications [reviewed in³⁹], which may affect its stability and the binding of co-factors and co-activators^{40,41}. Additionally, nuclear retention of ChREBP's mRNA⁴², and sequestration of ChREBP's heterodimer partner, Mlx, in lipid droplets play important roles in regulating ChREBP activity⁴³. Furthermore,



there are other mechanisms that have not been fully explored that may regulate the ratio of ChREBP isoform activity during increasing metabolic stress including differential mRNA and protein stability and differential protein translation rates. Clearly, a transcription factor that plays such an important role in beta cell function, proliferation, and apoptosis should be tightly controlled.

We have previously shown that the induction of ChREBP β is necessary for a full transcriptional and proliferative response to glucose in rodent β -cells *in vitro*¹⁰. Here we show that ChREBP β is necessary for adaptive β -cell proliferation and expansion of β -cell mass using models that remove ChREBP β either conditionally in adults, or embryonically. One important observation is that removal

Fig. 6 | Overexpression of ChREBP β leads to β -cell death, glucose intolerance and diabetes. **a** LSL-ChREBP β mice were bred with MIP-Cre-ERT mice to generate inducible β -cell-specific overexpressing ChREBP β mice, termed i β OE β (created with BioRender.com; see also Supplementary Figs 16 and 17). Presented are measurements from male mice (see also Supplementary Fig. 18 for female mice). **b, c** Glucose tolerance test and area under the curve (AUC) one week after vehicle oil or tamoxifen treatment. **d** Weekly measures of whole body weight. **e** Plasma Insulin levels after one week. **f** Non-fasting blood glucose levels for the indicated times and treatment groups. **g** β -cell mass (BCM) one week after vehicle oil or

tamoxifen treatment. **h, i** Glucose tolerance test and area under the curve (AUC) one month after vehicle oil or tamoxifen treatment. **j** β -cell mass (BCM) one month after vehicle oil or tamoxifen treatment. Data are means \pm SEM, $N = 4-6$; * $p < 0.05$; ** $P < 0.001$; **** $P < 0.0001$ using two-way ANOVA. **k, l** Percent Ki67-positive and insulin-positive cells in pancreata from male homozygous i β OE β mice 1 week after oil or tamoxifen injection. **m, n** Percent TUNEL-positive and insulin-positive cells in pancreata from male homozygous i β OE β mice 1 week after oil or tamoxifen treatment. Data are means \pm SEM from five mice/group. * $p < 0.05$ using two-way ANOVA.

of ChREBP β did not affect glucose homeostasis unless the mouse was challenged with a HFD. Thus, ChREBP β is dispensable for normal β -cell development and β -cell function under non-stressed circumstances. This is consistent with observations of very low expression levels of ChREBP β mRNA in β -cells cultured in low glucose and with global ChREBP knock out mice, which display relatively normal β -cell function^{10,44}. Another striking observation was that deletion of ChREBP β protected β -cells from glucolipotoxic cell death. Since ChREBP is lipogenic, and inhibition of lipogenesis promotes fatty acid oxidation and protection from ceramide-mediated β -cell death^{19,45,46}, a reasonable explanation for the protective effect of ChREBP β depletion in β -cells may be decreased lipogenesis and an increased ability to process the exogenous palmitate.

Whereas overexpression of ChREBP α does not cause cell death^{5,8}, overexpression of ChREBP β resulted in robust β -cell apoptosis, resulting in decreased β -cell mass and diabetes. As with our studies, Chan and colleagues found a similar result in INS-1 cells overexpressing a constitutively active version of ChREBP that lacks the LID domain and thus is functionally and structurally similar to ChREBP β ¹⁴. That ChREBP β drives apoptosis is consistent with the fact that *Txnip* is a target gene of ChREBP and that depleting β -cells of ChREBP or *Txnip* prevents glucotoxic mediated cell death^{7,14,47}. It seems that the ratio of ChREBP β to ChREBP α is critical for β -cell fate, and that a threshold of ChREBP β must be reached for pathological results to occur. We observed a dose- and time-dependent component of ChREBP β -mediated β -cell death in vivo, FACs-sorted human β -cells from T2D donors displayed a higher ChREBP β :ChREBP α ratio than from non-diabetic donors, and increasing the ChREBP α abundance mitigated ChREBP β -mediated cell death in vitro and in vivo in both rodent and human β -cells. These results are in concert with studies showing high levels of ChREBP correlate with poor diagnosis and increased rates of proliferation in certain forms of cancer⁴⁸. Indeed, in many respects, ChREBP β behaves very much like Myc in β -cells. Myc is induced by glucose and its overexpression is closely correlated to glucose toxicity and the reduction of β -cell-enriched genes, including insulin itself⁴⁹. Furthermore, overexpression of ChREBP β , much like Myc, results in a general amplification of actively transcribed genes^{31,50}. Collectively, these results suggest that ChREBP α and ChREBP β drive different transcriptional programs. On the one hand, overexpression of both ChREBP α and ChREBP β result in decreased expression of β -cell markers [ref. 51 and this study]. On the other hand, overexpression of ChREBP β leads to hyper-expression of *Txnip* and cell death, whereas overexpression of ChREBP α activates the Nrf2 antioxidant pathway via unknown mechanism, resulting in enhanced glucose-stimulated proliferation and protection from ChREBP β -mediated cell death [ref. 8 and this study]. The identity of the different gene targets of the two ChREBP isoforms and the mechanisms by which they are regulated are areas of active investigation.

Interestingly, Shalev and colleagues demonstrated that ChREBP β overexpression decreases ChREBP α abundance and postulated that a role of ChREBP β is to prevent ChREBP α from mediating glucose toxicity¹³. Those experiments were performed at relatively early time points in vitro and did not assess apoptosis. We suspect that had

longer term experiments in the studies of Jing et al. would have revealed results similar to those reported here.

We found it possible to mitigate the effect of ChREBP β by either restoring the balanced ratio of ChREBP β to ChREBP α , or by activating the Nrf2 antioxidant pathway. The latter effect follows from our previous study demonstrating that overexpression of ChREBP α results in the activation of Nrf2⁸. Considering that ChREBP β drives glucose toxicity, it is not surprising that activation of an antioxidant pathway alleviates its pathological effects. Glucose toxicity can be alleviated and β -cell function improved by a large variety of antioxidants, particularly those that activate the Nrf2 pathway¹⁵. Of note is the study by Kjørholt et al. demonstrating that hyperglycemia rather than hyperlipidemia leads to β -cell dedifferentiation and decreased insulin secretion in *db/db* mice, and a number of studies demonstrating that normalizing blood glucose levels with insulin or SGLT2 deletion improves β -cell function⁵²⁻⁵⁴. We suggest that these effects are likely due, in part, to cessation of the positive feedback loop producing ChREBP β and a restoration of the ChREBP α :ChREBP β ratio and redox balance.

A number of Nrf2 activators have been or are currently being tested in clinical trials for the treatment of diabetes. Bardoxolone methyl (CDDO-Me) was investigated for treatment of chronic kidney disease in people with diabetes, but this clinical trial was terminated early due to cardiovascular safety concerns⁵⁵. A new Phase II clinical trial with CDDO-Me has recently started, excluding at-risk patients⁵⁶. Several natural compounds that activate Nrf2 are also under clinical trials, though many have anti-inflammatory effects acting through pathways other than Nrf2, and point out the very real possibility of beneficial off target side effects⁵⁷. Clearly more studies are needed to improve tissue and target specificity of Nrf2 activator compounds before realizing their potential for increasing or preserving β -cell mass in diabetes.

We acknowledge that this study was limited to β -cells. It will be important to determine whether the mechanistic details of the positive feedback loop as described here apply to other tissues affected by glucose toxicity such as kidney, liver and adipose tissue. In addition, we did not define the exact mechanism of ChREBP β -mediated β -cell death. It will be important to understand how ChREBP β integrates with other mechanisms of glucose and lipid toxicity including ER stress, inflammasome activity, mitochondrial dysfunction and dysregulation of Foxo1⁵⁸⁻⁶¹.

In summary, we have clarified the role of ChREBP in β -cells by examining the unique functions of the two major forms of ChREBP, ChREBP α and ChREBP β . Developing tools that distinguish the two isoforms has allowed a precise delineation of the molecular mechanism by which glucose initiates a positive feedback loop that allows ChREBP β to become the major nuclear isoform of ChREBP in the context of adaptive responses such as from a HFD. Loss-of-function studies revealed that ChREBP β is necessary for adaptive expansion. However, excessive ChREBP β , as may happen from hyper-activation of the positive feedback loop with prolonged hyperglycemia or diabetes, results in β -cell apoptosis. Mitigation of ChREBP β toxicity is possible by addition of ChREBP α to restore ChREBP α :ChREBP β ratio, or by activation of the Nrf2 antioxidant pathway.

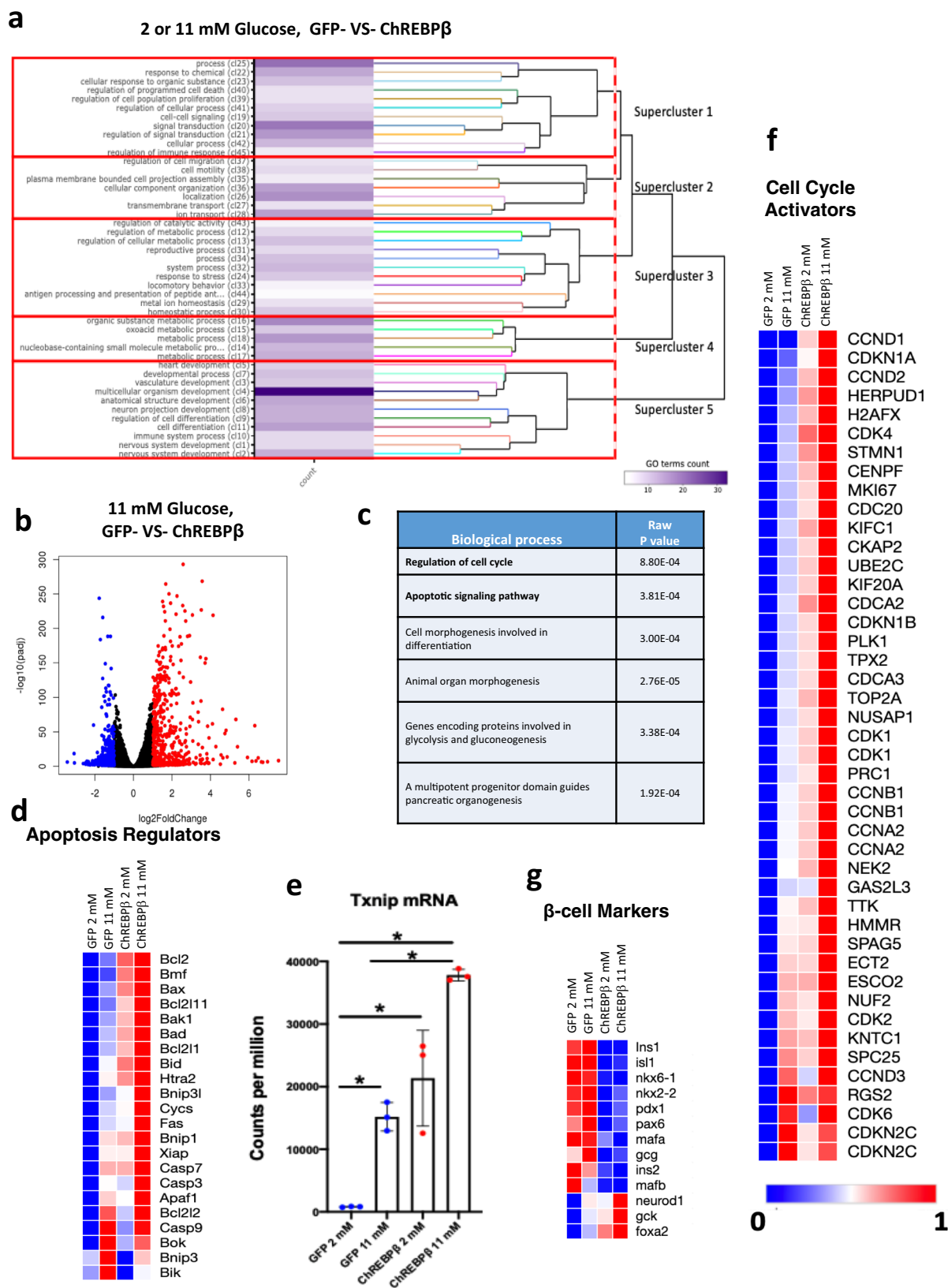


Fig. 7 | ChREBP β initiates programs of cell cycle regulation and apoptosis when overexpressed in Ins-1 cells. Ins-1 cells were transduced with an adenovirus expressing GFP or ChREBP β and cultured for 48 h in 2 or 11 mM glucose. RNA was collected and RNA-seq was performed. **a** Heatmap of the cluster of GO terms. The 471 GO terms (pathways) enriched by differentially expressed genes across the 6 DGEs from the 4 groups (see text) are grouped into 45 clusters of GO terms. The hierarchical tree scoring the distances between each of the 45 clusters originates superclusters that are boxed in red. The superclusters highlight the main cellular

functions common to the different DGEs. **b**, **c** Volcano plot and gene ontology of biological processes affected by ChREBP β compared to GFP-treated INS-1 cells cultured in 11 mM glucose. **d** Heat maps of the average expression levels of apoptosis regulators **e** *Txnip* mRNA expression; means of 3 independent measures, error bars are SEM; * $p < 0.05$. **f**, **g** Heat maps of the averages of differentially expressed cell cycle activators or β -cell marker genes. Values represent the average of three independent experiments and genes are sorted by the Pearson correlation of nearest neighbors.

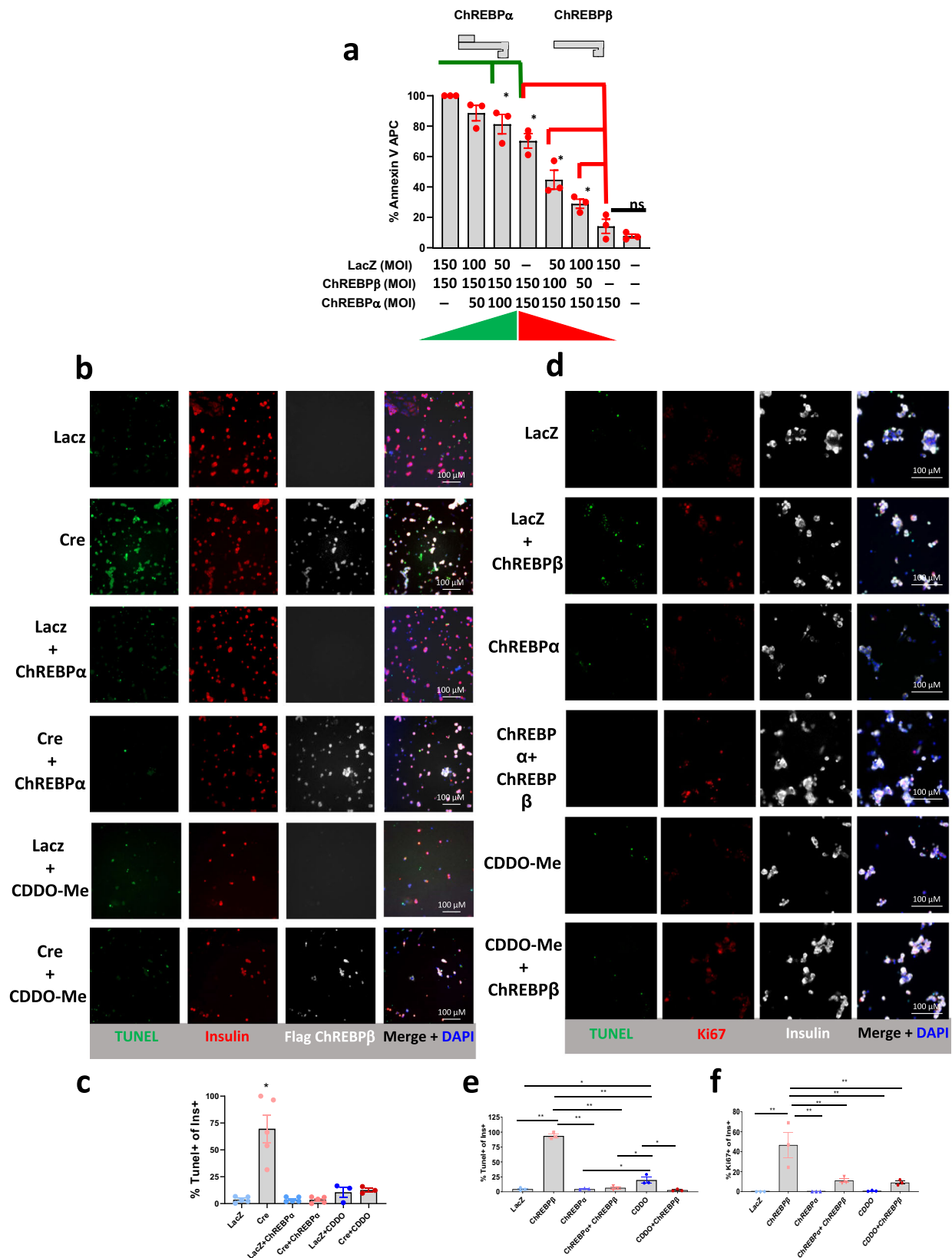


Fig. 8 | ChREBP α and activation of Nrf2 mitigates ChREBP β -mediated β -cell death. **a** The indicated amounts of ChREBP α and ChREBP β were transduced into INS-1-derived 832/13 cells and 48 h later apoptosis was measured with Annexin V staining. Error bars are SEM, $N = 3$, $*p < 0.05$. **b** Islets were isolated from Lox-Stop-Lox ChREBP β mice, dispersed and transduced with the indicated adenovirus or 10 μ M CDDO-Me for 48 h. Cells were immunostained or processed for TUNEL assay

as indicated. **c** Percent of TUNEL+/insulin+ cells from **(b)**. **d** Human islets were dispersed and transduced with the indicated adenovirus or 10 μ M CDDO-Me for 48 h and immunostained as indicated. **e** Percent of TUNEL+/insulin+ cells from **(d)**. **f** Percent of Ki67+/insulin+ cells from **(d)**. Data are the means \pm SEM, $n = 3-4$, $*p < 0.05$, $**p < 0.01$ using one-way ANOVA; ns not significant.

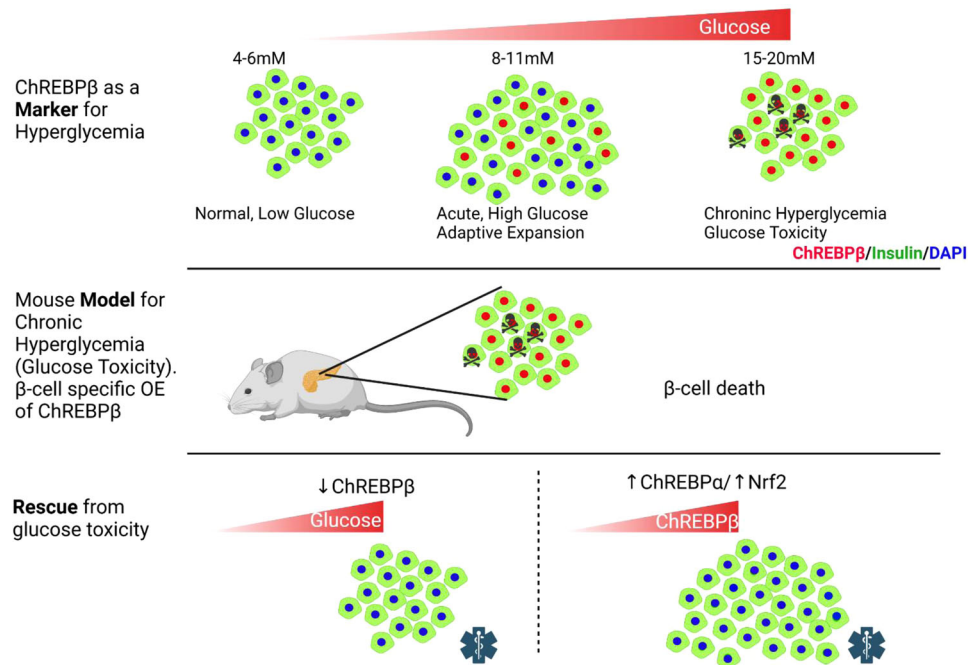


Fig. 9 | ChREBPβ is required for adaptive β-cell expansion but contributes to glucose toxicity with prolonged hyperglycemia and effects of its over-expression can be rescued by activation of the Nrf2 antioxidant pathway.

Nuclear expression of ChREBPβ increases in β-cells with increased glucose concentrations. Loss of function experiments demonstrate that ChREBPβ is necessary

for adaptive expansion of β-cells after a high fat diet. Gain of function experiments demonstrate that ChREBPβ overexpression mimics glucose toxicity. Deletion of ChREBPβ protects β-cells from glucolipotoxicity and ChREBPβ-mediated β-cell death can be mitigated by overexpression of ChREBPα or by activation of the Nrf2 antioxidant pathway. Created with BioRender.com.

Methods

Cell Culture

INS-1-derived 832/13 cells (a kind gift from Dr. Chris Newgard, Duke University)⁶² were cultured as described previously²¹. Mouse islets were isolated by Histopaque gradient following collagenase P injection to the pancreatic duct, as previously described⁶³. A day following the isolation islets were dispersed using 0.05% Trypsin. Islet cells were maintained in RPMI containing 5.5 mM glucose, 100 U/mL penicillin, 100 mg/mL streptomycin and 10% FCS as previously described⁶⁴. Human beta cells were isolated from human cadaveric islets donors provided by the NIH/NIDDK-supported Integrated Islet Distribution Program (IIDP) (<https://iidp.nih.gov/overview.aspx>), and from Prodo Labs (<https://prodolabs.com/>), the University of Miami, the University of Minnesota, the University of Wisconsin, the Southern California Islet Cell Resource center, and the University of Edmonton, as summarized in Supplementary Table 3. Informed consent was obtained by the Organ Procurement Organization (OPO), and all donor information was de-identified in accord with Institutional Review Board procedures at The Icahn School of Medicine at Mount Sinai (ISMMS). Human islets were cultured and dispersed as previously described⁵.

Adenovirus

Ins-1 cells, mouse islets or human islets were transduced with adenovirus at multiplicity of infection (MOI) of 150, unless otherwise indicated. Cells were seeded in RPMI with 100 U/mL penicillin, 100 mg/mL streptomycin in the presence of the virus for 16 h. The following day, FBS was added to a final concentration of 10% and glucose concentration was adjusted to the concentration of the treatment. Cells were harvested or fixed 72 h after transduction and 56 h in the noted glucose concentrations. Flag-tagged mouse ChREBPα and mCherry tagged mouse ChREBPβ were cloned into pDEST and adenoviruses were generated in HEK293 cells (ATCC cat# CRL-3216) as previously

described⁶⁵; ChREBP cDNAs were kind gift from Dr. Howard Towle (U. of Minnesota). The Nrf2 adenovirus was previously described in⁸.

Immunofluorescence

After islet dispersal with 0.05% trypsin, cells were plated on 12-mm laminin coated glass coverslips placed in 24-well plates^{24,66}. Islet cells were either uninfected or transduced and cultured as described above at a MOI of 150 of the adenoviruses indicated. Cells were then rinsed with PBS and fixed in 4% paraformaldehyde, and β-cell proliferation was determined by immunolabeling for Ki67 and Insulin. Confocal images were acquired using the Zeiss LSM 880 Airyscan. For time course experiments, cells were in a temperature and CO₂ controlled chamber throughout the experiment. Images were taken at 10 min intervals for the first 2 h following by hourly acquisition for a total of 10 h. Nuclear quantifications were performed by counting the overlap of DAPI positive nuclei and the marked fluorophore. Approximately 150 cells were counted for every time point.

Antibodies used

Antibodies used were: anti-insulin guinea pig polyclonal at 1:000 from DAKO (cat# A0564, AB_10013624); anti-glucagon mouse monoclonal at 1:500 from Abcam (cat# ab10988, AB_297642); anti-ChREBP C-term rabbit polyclonal at 1:250 from Novus (cat # NB400-135, AB_10002435); ChREBP N-term rabbit polyclonal at 1:250 generated by Genscript and validated in Supplementary Fig. 3; anti-Flag rabbit polyclonal at 1:500 from Cell Signaling (cat# 2368S, AB_2217020); Anti-green fluorescent protein (GFP) chicken polyclonal at 1:100 from Aves-Labs (cat# GFP-1020, AB_10000240); anti-Cherry (red fluorescent protein) rabbit polyclonal at 1:1000 from Rockland (cat# 600401379S, AB_11182807); anti-Ki67 rabbit monoclonal at 1:250 from ThermoScientific (cat# MA5-14520, AB_10979488), see Supplementary Table 2.

Genetically modified mice

Mice with β -Cell-specific inducible knockout or knockin of ChREBP β were generated by combining either MIP-CreERT mice²⁵ or RIP-Cre^{fl^{trr}} mice [ref. 26, MMRC-Jackson Labs] with floxed ChREBP β mice¹⁰ or with 3xFlag-tagged ChREBP β transgenic mice, respectively. To generate 3xFlag-tagged ChREBP β transgenic mice, a murine 3xFlag-tagged ChREBP β transgene was subcloned into a modified Rosa26-pCAG-LSL-WPRE-bGHpA targeting vector between the LSL and WPRE sequences⁶⁷. The LSL sequence contains loxP- Stop codons - 3x SV40 polyA - loxP. The targeting vector was linearized and transfected into the 129/B6 F1 ES cell line G4. G418-resistant ES clones were screened by PCR. Positive ES clones were injected into C57BL/6J blastocysts in the Boston Nutrition Obesity Research Center Transgenic Core to obtain chimeric mice following standard procedures. Chimeric mice were bred with C57BL/6J mice to obtain germline transmitted F1 mice and these mice were backcrossed onto the C57BL/6J background for more than 10 generations. All mice used in this study were in a C57BL/6J mouse background. Mice were periodically outbred to C57BL/6 to avoid off target effects and to minimize growth hormone effects caused by breeding the Cre allele to homozygosity, as well as to obtain Cre-negative littermate controls⁶⁸. Cre-mediated recombination was achieved by intraperitoneal injection for 5 consecutive days of 75 μ g/g body weight of tamoxifen (Tam) (Sigma-Aldrich) dissolved in corn oil. All protocols were performed with the approval of and in accordance with guidelines established by the Icahn School of Medicine at Mount Sinai Institutional Animal Care and Use Committee.

Islet transplantation

Human islets were transplanted into the renal subcapsular space as described previously^{24,66,69}. Numbers of human islet equivalents are described in the Figure Legends.

HFD feeding

14 week-old mice were fed with a lard-based HFD (41% kcal from fat) (TD 96001; Harlan Teklad) or a regular diet (RD) (13.1% kcal from fat) (Purina PicoLab 5053; LabDiet). After 7 or 30 days, body weights, non-fasting blood glucose, and plasma insulin were measured and pancreata harvested and processed for histological studies or islet isolation.

Glucose homeostasis

Blood glucose was determined by glucometer (AlphaTrack 2) and plasma insulin by ELISA (Mercodia). An intraperitoneal glucose tolerance test was performed in mice fasted for 16–18 h and injected intraperitoneally with 2 g d-glucose/kg. Insulin tolerance test was performed in non-fasted mice IP-injected with human insulin (1.5 units/kg). Glucose-stimulated insulin secretion and insulin measures were performed as previously described^{24,70}.

Immunohistochemistry and analysis of β -cell proliferation and mass

Paraffin-embedded pancreas sections were immunolabeled with antibodies for insulin (Dako) and Ki67 (Thermo Fisher Scientific), and at least 2000 β -cells were blindly counted per mouse. β -cell mass was measured from at least three insulin-labeled pancreas sections per mouse, at least 5 μ m from each other, and quantified using ImageJ (National Institutes of Health). For 3D pancreatic imaging, tissue was cleared using the iDISCO method for tissue clearing as previously described⁷¹. Z-stack images of insulin-positive pancreata were acquired using Ultramicroscope II (LightSheet) 3D reconstitution of the images and quantification of beta cell mass using Imaris (9.7.2) software.

Generation of CRISPR/Cas9 INS-1 cells

INS-1 cells were transfected with Lipofectamine 2000 (Invitrogen) according to the manufacturer's recommendations using two

plasmids: the first was the pX330 (Addgene) to which the PAM containing oligos were ligated into *BbsI* sites using T4 ligase (Promega, overnight according to manufacturer's instructions). For tagging the N-terminus of ChREBP, the guide RNA was constructed using the following primers: forward CACCGTTCGTCGCCAGCCCGGATTCGG and reverse AAACCCGAATCCGGGTCGGGACGACC. For tagging the C-terminus of ChREBP, the guide RNA was constructed using the following primers: forward CACCGACACGTCCCTCTCGATCCTGG and reverse AAACCCAGGATCGAGAGGGACGTGTCC. The first plasmid was co-transfected along with a second plasmid (pUC57) containing homology arms and the sequence for mCherry or eGFP, which was generated using GeneScript gene synthesis (sequence available upon request). Cells were allowed to recover after transfection and were expanded for 7–10 days after which they were collected by fluorescence-activated cytometric sorting at the Mount Sinai Flow Cytometry Core to isolate the fluorescent population of cells. The sorted population of cells was transfected as before, and the cycle of transfection and sorting was repeated 2–3 times to obtain a homogenous population of INS-1 cells expressing the desired fluorescent protein fused to endogenous ChREBP.

TUNEL and Annexin V assays

TUNEL labeling was performed according to the manufacturer, using the DeadEnd Fluorometric TUNEL System (Cat#G3250, Promega). Annexin V and PI staining were performed as described previously⁷² to distinguish dead (PI-AnnexinV+) and dying INS-1 cells (PI-AnnexinV+) from live INS-1 cells (PI-AnnexinV).

RNA Seq

Total RNA from $\sim 1 \times 10^6$ INS-1 cells was isolated using the RNeasy mini kit (Qiagen) according to the manufacturer's protocol. RNA integrity was assessed using Ribogreen to determine total mass and Fragment Analyzer was used to determine RNA integrity. All samples passed quality control, with RNA integrity scores are ranging from 7.7 to 10. Samples were submitted to Genewiz and RNA was amplified via the NuGEN Ovation RNA-Seq System V2 prior to RNA sequencing. Each sample was sequenced on a HiSeq2500 instrument (Illumina) at a depth of 35–40 million, 150 bp paired-end reads, that were single-indexed per lane. Raw counts were processed for DGE analysis using the edgeR R package (version 4.2), using a minimum fold change of 1.2. Six DGEs were conducted to reflect each possible comparison of the 4 groups. The resulting lists of differentially expressed genes were fed into the ViSEAGO R package (version 1.8.0). ViSEAGO carries out a data mining of biological functions and establishes links between genes involved in the study facilitating functional GO analysis of complex experimental design with multiple comparisons²⁹. For human studies, β -cells from dispersed human islets were transduced with an adenovirus expressing ZsGreen driven by a MIP-miniCMV promoter and harvested by fluorescence-activated cytometric sorting (FACS Aria II) as described previously^{22,66}. The β -cell fraction was confirmed to be >92% pure by immunolabeling of sorted cells with insulin, by qRT-PCR and by RNAseq⁶⁶. RNA sequencing, alignment and feature quantitation was as previously described²². The datasets generated during and/or analyzed during the current study are available in the GEO repository as accession number GSE197864.

qPCR and PCR

mRNA was isolated using the Qiagen RNeasy mini kit for INS-1 cells, or for islets using the Qiagen RNeasy mini kit. cDNA was produced using the Promega m-MLV reverse transcriptase. qPCR was performed on the QuantStudio5 using Syber-Green (BioRad) and analysis was performed using the $\Delta\Delta$ Ct method. PCR for genotyping was performed using standard methods. Primer sequences are shown in Supplementary Table 1.

Western blotting and chromatin immunoprecipitation

Cells were lysed in RIPA buffer (Thermo-Fisher) with protease inhibitors (Roche). Lysates were sonicated for 20 s on ice and centrifuged at $10,000 \times g$ for 5 min. Lysates were then placed in a 95°C for 5 min with Laemmli loading buffer. A total of $40 \mu\text{g}$ protein extract/well was loaded on 7.5% SDS polyacrylamide gels. Western blots were carried out using antibodies described in Supplementary Table 2, and the blots were scanned with the LI-COR laser-based image detection method as previously described⁷³. Chromatin immunoprecipitation was performed as previously described²¹.

Statistics

All studies were performed with a minimum of three independent repetition. Data presented in this study as means \pm standard error of the mean (SEM). Statistical analysis was performed using Two-way ANOVA on GraphPad (Prism) V9.2.

Reporting summary

Further information on research design is available in the Nature Research Reporting Summary linked to this article.

Data availability

The datasets generated during and/or analyzed during the current study are available in the GEO repository as accession number [GSE197864](https://www.ncbi.nlm.nih.gov/geo/query/acc.cgi?acc=GSE197864). Source data are provided with this paper.

References

- Wang, P. et al. Diabetes mellitus—advances and challenges in human beta-cell proliferation. *Nat. Rev. Endocrinol.* **11**, 201–212 (2015).
- Wang, P. et al. Human beta cell regenerative drug therapy for diabetes: past achievements and future challenges. *Front. Endocrinol.* **12**, 671946 (2021).
- Porat, S. et al. Control of pancreatic beta cell regeneration by glucose metabolism. *Cell Metab.* **13**, 440–449 (2011).
- Robertson, R. P., Harmon, J., Tran, P. O. & Poitout, V. Beta-cell glucose toxicity, lipotoxicity, and chronic oxidative stress in type 2 diabetes. *Diabetes* **53**, S119–S124 (2004).
- Metukuri, M. R. et al. ChREBP mediates glucose-stimulated pancreatic beta-cell proliferation. *Diabetes* **61**, 2004–2015 (2012).
- Yamashita, H. et al. A glucose-responsive transcription factor that regulates carbohydrate metabolism in the liver. *Proc. Natl Acad. Sci. USA* **98**, 9116–9121 (2001).
- Shalev, A. Minireview: Thioredoxin-interacting protein: regulation and function in the pancreatic β -cell. *Mol. Endocrinol.* **28**, 1211–1220 (2014).
- Kumar, A. et al. Activation of Nrf2 is required for normal and ChREBP α -augmented glucose-stimulated beta-cell proliferation. *Diabetes* **67**, 1561–1575 (2018).
- Herman, M. A. & Kahn, B. B. Glucose transport and sensing in the maintenance of glucose homeostasis and metabolic harmony. *J. Clin. Invest.* **116**, 1767–1775 (2006).
- Zhang, P. et al. Induction of the ChREBP β isoform is essential for glucose-stimulated beta cell proliferation. *Diabetes* **64**, 4158–4170 (2015).
- Herman, M. A. et al. A novel ChREBP isoform in adipose tissue regulates systemic glucose metabolism. *Nature* **484**, 333–338 (2012).
- Sae-Lee, C., Moolsuwan, K., Chan, L. & Pongvarin, N. ChREBP regulates itself and metabolic genes implicated in lipid accumulation in β -cell line. *PLoS ONE* **11**, e0147411 (2016).
- Jing, G., Chen, J., Xu, G. & Shalev, A. Islet ChREBP- β is increased in diabetes and controls ChREBP- α and glucose-induced gene expression via a negative feedback loop. *Mol. Metab.* **5**, 1208–1215 (2016).
- Pongvarin, N. et al. Carbohydrate response element-binding protein (ChREBP) plays a pivotal role in beta cell glucotoxicity. *Diabetologia* **55**, 1783–1796 (2012).
- Baumel-Alterzon, S. et al. Nrf2 Regulates β -Cell Mass by Suppressing β -Cell Death and Promoting β -Cell Proliferation. *Diabetes* **71**, 989–1011 (2022).
- Cha-Molstad, H., Saxena, G., Chen, J. & Shalev, A. Glucose-stimulated expression of Txnip is mediated by carbohydrate response element-binding protein, p300, and histone H4 acetylation in pancreatic beta cells. *J. Biol. Chem.* **284**, 16898–16905 (2009).
- Davies, M. N., O’Callaghan, B. L. & Towle, H. C. Glucose activates ChREBP by increasing its rate of nuclear entry and relieving repression of its transcriptional activity. *J. Biol. Chem.* **283**, 24029–24038 (2008).
- Noordeen, N. A., Meur, G., Rutter, G. A. & Leclerc, I. Glucose-induced nuclear shuttling of ChREBP is mediated by sorcin and Ca(2+) ions in pancreatic beta-cells. *Diabetes* **61**, 574–585 (2012).
- Abdul-Wahed, A., Guilmeau, S. & Postic, C. Sweet sixteenth for ChREBP: established roles and future goals. *Cell Metab.* **26**, 324–341 (2017).
- Stoeckman, A. K., Ma, L. & Towle, H. C. Mlx is the functional heteromeric partner of the carbohydrate response element-binding protein in glucose regulation of lipogenic enzyme genes. *J. Biol. Chem.* **279**, 15662–15669 (2004).
- Zhang, P. et al. c-Myc is required for the ChREBP-dependent activation of glucose-responsive genes. *Mol. Endocrinol.* **24**, 1274–1286 (2010).
- Wang, H. et al. Insights into beta cell regeneration for diabetes via integration of molecular landscapes in human insulinomas. *Nat. Commun.* **8**, 767 (2017).
- Gómez-Banoy, N. et al. Adipsin preserves beta cells in diabetic mice and associates with protection from type 2 diabetes in humans. *Nat. Med.* **25**, 1739–1747 (2019).
- Wang, P. et al. A high-throughput chemical screen reveals that harmine-mediated inhibition of DYRK1A increases human pancreatic beta cell replication. *Nat. Med.* **21**, 383–388 (2015).
- Wicksteed, B. et al. Conditional gene targeting in mouse pancreatic β -cells: analysis of ectopic Cre transgene expression in the brain. *Diabetes* **59**, 3090–3098 (2010).
- Herrera, P. L., Orci, L. & Vassalli, J. D. Two transgenic approaches to define the cell lineages in endocrine pancreas development. *Mol. Cell. Endocrinol.* **140**, 45–50 (1998).
- Collier, J. J. et al. c-Myc and ChREBP regulate glucose-mediated expression of the L-type pyruvate kinase gene in INS-1-derived 832/13 cells. *Am. J. Physiol. Endocrinol. Metab.* **293**, E48–E56 (2007).
- Rosselot, C. et al. Myc is required for adaptive beta-cell replication in young mice but is not sufficient in one-year-old mice fed with a high-fat diet. *Diabetes* **68**, 1934–1949 (2019).
- Brionne, A., Juanchich, A. & Hennequet-Antier, C. ViSEAGO: a Bioconductor package for clustering biological functions using Gene Ontology and semantic similarity. *BioData Min.* **12**, 16 (2019).
- Chen, J., Saxena, G., Mungrue, I. N., Lusic, A. J. & Shalev, A. Thioredoxin-interacting protein: a critical link between glucose toxicity and beta-cell apoptosis. *Diabetes* **57**, 938–944 (2008).
- Nie, Z. et al. c-Myc is a universal amplifier of expressed genes in lymphocytes and embryonic stem cells. *Cell* **151**, 68–79 (2012).
- Puri, S. et al. Replication confers beta cell immaturity. *Nat. Commun.* **9**, 485 (2018).
- Sharma, R. B., Darko, C., Zheng, X., Gablaski, B. & Alonso, L. C. DNA damage does not cause BrdU labeling of mouse or human β -cells. *Diabetes* **68**, 975–987 (2019).
- Rieck, S. & Kaestner, K. H. Expansion of beta-cell mass in response to pregnancy. *Trends Endocrinol. Metab.* **21**, 151–158 (2010).

35. Robertson, R. P. Chronic oxidative stress as a central mechanism for glucose toxicity in pancreatic islet beta cells in diabetes. *J. Biol. Chem.* **279**, 42351–42354 (2004).
36. Weir, G.C., Butler, P.C. & Bonner-Weir, S. The β -cell glucose toxicity hypothesis: attractive but difficult to prove. *Metabolism* **124**, 154870 (2021).
37. Park, M. J. et al. High glucose-induced O-GlcNAcylated carbohydrate response element-binding protein (ChREBP) mediates mesangial cell lipogenesis and fibrosis: the possible role in the development of diabetic nephropathy. *J. Biol. Chem.* **289**, 13519–13530 (2014).
38. Agius, L., Chachra, S. S. & Ford, B. E. The protective role of the carbohydrate response element binding protein in the liver: the metabolite perspective. *Front Endocrinol. (Lausanne)* **11**, 594041 (2020).
39. Katz, L. S., Baumel-Alterzon, S., Scott, D. K. & Herman, M. A. Adaptive and maladaptive roles for ChREBP in the liver and pancreatic islets. *J. Biol. Chem.* **296**, 100623 (2021).
40. Bricambert, J. et al. The histone demethylase Phf2 acts as a molecular checkpoint to prevent NAFLD progression during obesity. *Nat. Commun.* **9**, 2092 (2018).
41. Lane, E. A. et al. HCF-1 regulates de novo lipogenesis through a nutrient-sensitive complex with ChREBP. *Mol. Cell* **75**, 357–371.e357 (2019).
42. Bahar Halpern, K. et al. Nuclear retention of mRNA in mammalian tissues. *Cell Rep.* **13**, 2653–2662 (2015).
43. Mejhert, N. et al. Partitioning of MLX-family transcription factors to lipid droplets regulates metabolic gene expression. *Mol. Cell* **77**, 1251–1264.e1259 (2020).
44. Iizuka, K., Bruick, R. K., Liang, G., Horton, J. D. & Uyeda, K. Deficiency of carbohydrate response element-binding protein (ChREBP) reduces lipogenesis as well as glycolysis. *Proc. Natl Acad. Sci. USA* **101**, 7281–7286 (2004).
45. Shimabukuro, M., Zhou, Y. T., Levi, M. & Unger, R. H. Fatty acid-induced beta cell apoptosis: a link between obesity and diabetes. *Proc. Natl Acad. Sci. USA* **95**, 2498–2502 (1998).
46. Gonzalez-Pertusa, J. A. et al. Novel proapoptotic effect of hepatocyte growth factor: synergy with palmitate to cause pancreatic β -cell apoptosis. *Endocrinology* **151**, 1487–1498 (2010).
47. Shalev, A. Lack of TXNIP protects beta-cells against glucotoxicity. *Biochemical Soc. Trans.* **36**, 963–965 (2008).
48. Lei, Y., Zhou, S., Hu, Q., Chen, X. & Gu, J. Carbohydrate response element binding protein (ChREBP) correlates with colon cancer progression and contributes to cell proliferation. *Sci. Rep.* **10**, 4233 (2020).
49. Laybutt, D. R. et al. Overexpression of c-Myc in beta-cells of transgenic mice causes proliferation and apoptosis, down-regulation of insulin gene expression, and diabetes. *Diabetes* **51**, 1793–1804 (2002).
50. Lin, C. Y. et al. Transcriptional amplification in tumor cells with elevated c-Myc. *Cell* **151**, 56–67 (2012).
51. da Silva Xavier, G., Sun, G., Qian, Q., Rutter, G. A. & Leclerc, I. ChREBP regulates Pdx-1 and other glucose-sensitive genes in pancreatic β -cells. *Biochem. Biophys. Res. Commun.* **402**, 252–257 (2010).
52. Jurczak, M. J. et al. SGLT2 deletion improves glucose homeostasis and preserves pancreatic beta-cell function. *Diabetes* **60**, 890–898 (2011).
53. Kjærholt, C., Akerfeldt, M. C., Biden, T. J. & Laybutt, D. R. Chronic hyperglycemia, independent of plasma lipid levels, is sufficient for the loss of beta-cell differentiation and secretory function in the db/db mouse model of diabetes. *Diabetes* **54**, 2755–2763 (2005).
54. Wang, Z., York, N. W., Nichols, C. G. & Remedi, M. S. Pancreatic beta cell dedifferentiation in diabetes and redifferentiation following insulin therapy. *Cell Metab.* **19**, 872–882 (2014).
55. de Zeeuw, D. et al. Bardoxolone methyl in type 2 diabetes and stage 4 chronic kidney disease. *N. Engl. J. Med.* **369**, 2492–2503 (2013).
56. Toto, R. D. Bardoxolone-the Phoenix? *J. Am. Soc. Nephrology* **29**, 360–361 (2018).
57. Baumel-Alterzon, S., Katz, L.S., Brill, G., Garcia-Ocaña, A. & Scott, D. K. Nrf2: The master and captain of beta cell fate. *Trends Endocrinol. Metab.* **32**, 7–19 (2020).
58. Schroder, K., Zhou, R. & Tschopp, J. The NLRP3 inflammasome: a sensor for metabolic danger? *Science* **327**, 296–300 (2010).
59. Talchai, C., Xuan, S., Lin, H. V., Sussel, L. & Accili, D. Pancreatic beta cell dedifferentiation as a mechanism of diabetic beta cell failure. *Cell* **150**, 1223–1234 (2012).
60. Wali, J. A. et al. The proapoptotic BH3-only proteins Bim and Puma are downstream of endoplasmic reticulum and mitochondrial oxidative stress in pancreatic islets in response to glucotoxicity. *Cell Death Dis.* **5**, e1124 (2014).
61. Wang, H., Kouri, G. & Wollheim, C. B. ER stress and SREBP-1 activation are implicated in beta-cell glucolipotoxicity. *J. Cell Sci.* **118**, 3905–3915 (2005).
62. Hohmeier, H. E. et al. Isolation of INS-1-derived cell lines with robust ATP-sensitive K⁺ channel-dependent and -independent glucose-stimulated insulin secretion. *Diabetes* **49**, 424–430 (2000).
63. Ricordi, C. & Rastellini, C. In: *Methods in Cell Transplantation* (ed. Ricordi, C.). (R. G. Landes, 1995).
64. Garcia-Ocana, A. et al. Transgenic overexpression of hepatocyte growth factor in the beta-cell markedly improves islet function and islet transplant outcomes in mice. *Diabetes* **50**, 2752–2762 (2001).
65. Becker, T. C. et al. Use of recombinant adenovirus for metabolic engineering of mammalian cells. *Methods Cell Biol.* **43**, 161–189 (1994).
66. Wang, P. et al. Combined inhibition of DYRK1A, SMAD, and tri-thorax pathways synergizes to induce robust replication in adult human beta cells. *Cell Metab.* **29**, 638–652.e635 (2019).
67. Madisen, L. et al. Transgenic mice for intersectional targeting of neural sensors and effectors with high specificity and performance. *Neuron* **85**, 942–958 (2015).
68. Estall, J. L. & Srean, R. A. Of mice and men, redux: modern challenges in β cell gene targeting. *Endocrinology* **161**, bqaa078 (2020).
69. Acefifi, C. et al. GLP-1 receptor agonists synergize with DYRK1A inhibitors to potentiate functional human β cell regeneration. *Sci. Transl. Med.* **12**, eaaw9996 (2020).
70. Lakshminpathi, J. et al. PKC-zeta is essential for pancreatic beta cell replication during insulin resistance by regulating mTOR and cyclin-D2. *Diabetes* **65**, 1283–1296 (2016).
71. Alvarsson, A. et al. A 3D atlas of the dynamic and regional variation of pancreatic innervation in diabetes. *Sci. Adv.* **6**, eaaz9124 (2020).
72. Davenport, B. et al. Aging of antiviral CD8(+) memory T cells fosters increased survival, metabolic adaptations, and lymphoid tissue homing. *J. Immunol.* **202**, 460–475 (2019).
73. Katz, L. S., Xu, S., Ge, K., Scott, D. K. & Gershengorn, M. C. T3 and glucose coordinately stimulate ChREBP-mediated Ucp1 expression in brown adipocytes from male mice. *Endocrinology* **159**, 557–569 (2018).

Acknowledgements

D.K.S., R01DK108905, R01DK114338, R01DK130300; J.C.L., R01DK12140; A.F.S., R01DK116873, R01DK125285, R01DK129196; A.G.-O., R01DK125285, R01DK105015, R01DK126450; A.A., Charles H. Revson Foundation (grant no. 18-25), Sweden-America Foundation (Ernst O Eks fond), Swedish Society for Medical Research (SSMF); S.S., American Diabetes Association Pathway to Stop Diabetes Grant ADA #1-17-ACE-31, R01NS097184, OT2OD024912, and R01DK124461, Department of

Defense (W81XWH-20-1-0345, W81XWH-20-1-0156); D.H., R01AG026518 and R01AI093637, Juvenile Diabetes Research Foundation Career Development Award 2-2007-240; (B.D.) T32 DK007792; MAH, R01DK100425. We thank the Boston Nutrition Obesity Research Center for generation of mice. We thank the Flow Cytometry, Microscopy, Mouse Genetics and Gene Targeting, the Biorepository and Pathology Cores of Icahn School of Medicine at Mount Sinai. We also thank the Human Islet and Adenovirus Core of the Einstein-Mount Sinai Diabetes Research Center (DK-020541) for generation of adenoviruses and islet transplantation services. We thank Pedro Herrera and Daniel Oropeza for useful discussions.

Author contributions

Conceptualization, L.S.K., and D.K.S.; Methodology, L.S.K., A.A., S.A.S., B.D., D.H., P.W., L.D., and M.A.H.; Investigation, L.S.K., G.B., P.Z., A.K., S.B.-A., L.B.H., N.G.-B., E.K., and M.T.; Formal analysis, L.L.; Resources, N.G.-B., J.C.L., L.D., and M.A.H.; Writing—original draft, L.S.K., and D.K.S.; Writing—review and editing, L.S.K., D.S.K., A.F.S., and A.G.-O.; Supervision and funding acquisition, S.A.S., A.F.S., D.H., J.C.L., M.A.H., A.G.-O., and D.K.S.

Competing interests

The authors declare no competing interests.

Additional information

Supplementary information The online version contains supplementary material available at <https://doi.org/10.1038/s41467-022-32162-x>.

Correspondence and requests for materials should be addressed to Donald K. Scott.

Peer review information *Nature Communications* thanks Nika Danial and Isabelle Leclerc for their contribution to the peer review of this work. Peer reviewer reports are available.

Reprints and permission information is available at <http://www.nature.com/reprints>

Publisher's note Springer Nature remains neutral with regard to jurisdictional claims in published maps and institutional affiliations.

Open Access This article is licensed under a Creative Commons Attribution 4.0 International License, which permits use, sharing, adaptation, distribution and reproduction in any medium or format, as long as you give appropriate credit to the original author(s) and the source, provide a link to the Creative Commons license, and indicate if changes were made. The images or other third party material in this article are included in the article's Creative Commons license, unless indicated otherwise in a credit line to the material. If material is not included in the article's Creative Commons license and your intended use is not permitted by statutory regulation or exceeds the permitted use, you will need to obtain permission directly from the copyright holder. To view a copy of this license, visit <http://creativecommons.org/licenses/by/4.0/>.

© The Author(s) 2022, corrected publication 2022